

Journal: ACP

MS No.: acp-2018-1273

Title: Insight into the Composition of Organic Compounds ($\geq C_6$) in PM_{2.5} in Wintertime in Beijing, China

Author(s): Ruihe Lyu et al.

Special Issue: In-depth study of air pollution sources and processes within Beijing and its surrounding region (APHH-Beijing) (ACP/AMT inter-journal SI)

RESPONSE TO REVIEWER #2

Comments: This manuscript has been well improved and the authors have answered most of the questions. However, I still have one question regarding the conclusion of 'There is strong evidence that the organic aerosol is more highly oxidized ,...on haze days' in the abstract (Line 49-50). In line 534-537 'By definition, concentrations of PM_{2.5} are elevated during haze events, but the question arises as to whether primary or secondary organic compounds make a larger contribution to the rise in concentrations. Constituents that are expected to be primary are typically elevated in mean concentration by a factor of around two', it shows the higher primary contribution on haze days compared to non-haze days. In Line 376 'lower ratios of O-PAHs/PAHs on haze days than non-haze days were observed'. In line 549-554 'This result was consistent with Section 3.5; ...a low ratio may reflect a high degree of further processing to form more oxidised 553 species on the haze days compensating for enhanced formation'. These observation or discussion probably indicates that the organic aerosol on non-haze days are more oxidized. So, I'm doubting about the conclusion in the abstract. If this comment can be addressed, I am very happy to suggest this manuscript to be published in Atmos. Chem. Phys.

RESPONSE: We thank the reviewer for pointing out the apparent inconsistency. The statement in the abstract is based upon the distribution of compounds in the chromatogram, and the final sentence of the abstract has been amended to reflect this more clearly.

**Insight into the Composition of Organic Compounds
($\geq C_6$) in PM_{2.5} in Wintertime in Beijing, China**

**Ruihe Lyu^{1,2}, Zongbo Shi², Mohammed Salim Alam²,
Xuefang Wu^{2,4}, Di Liu², Tuan V. Vu², Christopher Stark²,
Pingqing Fu³, Yinchang Feng¹ and Roy M. Harrison^{2†*}**

**¹ State Environmental Protection Key Laboratory of Urban Ambient Air
Particulate Matter Pollution Prevention and Control, College of
Environmental Science and Engineering
Nankai University, Tianjin 300350, China**

**² Division of Environmental Health and Risk Management
School of Geography, Earth and Environmental Sciences, University of
Birmingham Edgbaston, Birmingham B15 2TT, UK**

**³ Institute of Surface Earth System Science, Tianjin University
Tianjin, 300350, China**

**⁴ Regional Department of Geology and Mineral Resources, China
University of Geosciences, Xueyuan Road 29, 100083 Beijing China**

**† Also at: Department of Environmental Sciences / Centre of Excellence in
Environmental Studies, King Abdulaziz University, PO Box 80203, Jeddah, 21589,
Saudi Arabia**

Corresponding author: E-mail: r.m.harrison@bham.ac.uk (Roy M. Harrison)

ABSTRACT

Organic matter is a major component of $\text{PM}_{2.5}$ in megacities. In order to understand the detailed characteristics of organic compounds ($\geq \text{C}_6$) at a molecular level on non-haze and haze days, we determined more than 300 organic compounds in the $\text{PM}_{2.5}$ from an urban area of Beijing collected in November-December 2016 using two-dimensional gas chromatography coupled to time-of-flight mass spectrometry ($\text{GC} \times \text{GC-TOFMS}$). The identified organic compounds have been classified into groups, and quantitative methods were used to calculate their concentrations. Primary emission sources make significant contributions to the atmospheric organic compounds and six groups (including n-alkanes, polycyclic aromatic hydrocarbons (PAHs), levoglucosan, branched-alkanes, n-alkenes and alkyl-benzenes) account for 66% of total identified organic compound mass. In addition, PAHs, and oxygenated PAHs (O-PAHs) were abundant amongst the atmospheric organic compounds on both haze and non-haze days. The most abundant hydrocarbon groups were observed with a carbon atom range of $\text{C}_{19}\text{-C}_{28}$. In addition, the total concentration of unidentified compounds present in the chromatogram was estimated in the present study. The total identified compounds account for approximately 47% of total organic compounds ($\geq \text{C}_6$) in the chromatogram on both the non-haze and haze days. The total mass concentrations of organic compounds ($\geq \text{C}_6$) in the chromatogram were $4.0 \mu\text{g m}^{-3}$ and $7.4 \mu\text{g m}^{-3}$ on the non-haze and haze days respectively, accounting for 26.4% and 18.5% of organic matter respectively on those days estimated from the total organic carbon concentration. Ratios of individual compound concentrations between haze and non-haze days do not give a clear indication of the degree of oxidation, but the overall distribution of organic compounds in the chromatogram provides strong evidence that the organic aerosol is less G.C.-volatile and hence more highly oxidised on haze days. Ratios of individual compound concentrations between haze and non-haze days do not give a clear indication of the degree of oxidation, but the overall distribution of organic compounds in the chromatogram provides strong evidence that the organic aerosol is less G.C.-volatile and hence more highly oxidised on haze days.

56 **Keywords:** Organic aerosol; GC \times GC-TOFMS; PAHs; Haze; PM_{2.5} Beijing, China

57

1. INTRODUCTION

China is suffering from severe PM_{2.5} pollution, especially in its capital, the annual average concentration of PM_{2.5} in Beijing being in the range 69.7~122 $\mu\text{g m}^{-3}$ from 2000 to 2015 (Lang et al., 2017), 2.0~3.5 times the national standard (35 $\mu\text{g m}^{-3}$). A recent study showed that the average PM_{2.5} concentration during the haze days was 256 $\mu\text{g m}^{-3}$ in the winter period from December 1, 2015 to December 31, 2015 in Beijing, and very much higher than that of non-haze days (24.7 $\mu\text{g m}^{-3}$) (Li, et al. 2019), and 25 times the World Health Organization (WHO) guideline of 10 $\mu\text{g m}^{-3}$.

Organic matter is a large and important fraction of atmospheric fine particles, and a substantial number of organic compounds can be found in the atmospheric particulate phase and may originate as either primary emissions or from secondary formation process (Wu et al., 2018). The primary emission tracers and precursor compounds have been extensively studied in the Beijing aerosol and showed significant contributions from coal combustion, biomass burning and traffic emissions (Ren et al., 2016; Yao et al., 2016). These studies concentrated on the identification of individual organic compounds from the organic aerosol, such as n-alkanes, n-alkenes, PAHs and hopanes, but the structurally specific identification of the chemical composition of the organic aerosol is far from complete. Due to its huge complexity, particulate organic matter is still inadequately characterized up to the present. Hence, the identification of organic compounds in generic groups may be more informative in elucidating the molecular distribution of atmospheric organic compounds, and bulk aerosol characteristics (Alam et al., 2018). Previous studies have shown that the organic compounds were highly oxidized during haze days, and secondary formation has made a significant contribution to the PM (Li et al., 2019). However, these studies focused only on specific individual oxidized organic compounds or the ratios of C, N and O to assess the entire aerosol ageing process (Li et al., 2019), and the relationship between the molecular distribution and oxidizing processes during haze formation is still not clear.

Two-dimensional gas chromatography (GC×GC) coupled with TOF-MS offers much enhanced resolution of complex mixtures, and the technique has been extended in the last 10 years to encompass atmospheric analysis. The two independent analytical dimensions in GC×GC-TOF/MS make this technique potentially ideal for measuring the organic components within a complex matrix such as ambient particulate matter (Hamilton et al., 2004; Welthagen et al., 2003), and its ability to separate complex mixtures of organics at low concentrations makes it an ideal technique to measure partially oxidised, isomeric and homologous series compounds and even groups of compounds (Alam et al., 2016a; Alam and Harrison, 2016; Hamilton et al., 2004). In an earlier study of organic compounds in the Beijing atmosphere, Zhou et al. (2009) reported that 68.4% of particulate organic matter was in the previously “unresolved complex mixture” found in conventional GC separations. The GC × GC technique is able to resolve and identify the components contributing to the unresolved mixture, and the molecular distribution of atmospheric organic compounds can be clearly identified in the chromatogram.

In order to establish relationships between organic compounds in fine particles and their characteristics on non-haze and haze days, as well as to identify the relative importance of their emission sources, further investigation of particulate organic matter composition has been conducted. The objective of this study was to investigate the organic compounds with carbon number higher than C₆ in PM_{2.5} samples collected in central Beijing during wintertime, 2016. In this paper, particle samples were analysed by the GC×GC-TOFMS technique after solvent extraction and the detailed organic composition was observed for polar and non-polar organic compound groups. Here, we report a large number of organic compounds, and their concentrations and molecular distributions sampled on non-haze and haze days. The characteristics of the molecular distribution of atmospheric organic compounds on non-haze days were analysed and compared with haze days during aerosol ageing. In addition, we report their possible sources, formation processes, and reveal and assess their pollution characteristics during non-haze and haze periods. Finally,

107 the mass of unidentified organic compounds ($>C_6$) is estimated and compared between non-haze and
108 haze days.

109

110 **2. MATERIALS AND METHODS**

111 **2.1 Sampling Method and Site Characteristics**

112 PM_{2.5} samples were collected at the Institute of Atmospheric Physics (IAP), Chinese Academy of
113 Sciences in Beijing, China. The sampling site (39°58'N, 116° 22'E) was located between the North 3rd
114 Ring Road and North 4th Ring Road. The site is approximately 1 km from the 3rd Ring Road, 200 m
115 west of the G6 Highway (which runs north-south) and 50 m south of Beitucheng West Road (which runs
116 east-west). The annual average vehicular speeds in the morning and evening traffic peak were 27.4 and
117 24.3 km h⁻¹, respectively. No industrial sources were located in the vicinity of the sampling site. The
118 experimental campaign took place from November 9 to December 11, 2016. The samples were collected
119 onto pre-baked quartz fibre filters (Pallflex) by a gravimetric high volume sampler (Tisch, USA) with a
120 PM_{2.5} inlet at a flow rate of 1.0 m³ min⁻¹ during the sampling period. The collecting time was 24 h per
121 sample and 3 blank samples were collected during this period. The filters were previously enveloped
122 with aluminium foils and then baked at 450 °C for 6 hours before sampling. After sampling, each filter
123 was packed separately and stored in a refrigerator below -20°C until the analysis.

124

125 **2.2 Analytical Instrumentation**

126 The sample extracts were analyzed using a 2D gas chromatograph (GC, 7890A, Agilent Technologies,
127 Wilmington, DE, USA) equipped with a Zoex ZX2 cryogenic modulator (Houston, TX, USA). The first
128 dimension was separated on a SGE DBX5, non-polar capillary column (30.0 m, 0.25 mm ID, 0.25 mm
129 – 5.00% phenyl polysilphenylene-siloxane), and the second-dimension column was a SGE DBX50 (4.0
130 m, 0.10 mm ID, 0.10 mm – 50.0% phenyl polysilphenylene-siloxane). The GC × GC was interfaced

with a Bench-ToF-Select, time-of-flight mass spectrometer (ToF-MS, Markes International, Llantrisant, UK). The acquisition speed was 50.0 Hz with a mass resolution of >1200 fwhm at 70.0 eV and the mass range was 35.0 to 600 m/z. All data produced were processed using GC Image v2.5 (Zoex Corporation, Houston, US).

2.3 Extraction and Analysis Methods of Filters

The filters were spiked with 30.0 μL of 30.0 $\mu\text{g mL}^{-1}$ deuterated internal standards (pentadecane- d_{32} , eicosane- d_{42} , pentacosane- d_{52} , triacontane- d_{62} , butylbenzene- d_{14} , nonylbenzene-2,3,4,5,6- d_5 , biphenyl- d_{10} , p-terphenyl- d_{14} ; Sigma-Aldrich, UK) for quantification and then immersed in methanol/dichloromethane (DCM) (1:1, v/v), and ultra-sonicated for 20 min at 20°C. The extract was filtered using a clean glass pipette column packed with glass wool and anhydrous Na_2SO_4 , and concentrated to 100 μL under a gentle flow of nitrogen for analysis using GC \times GC-ToF-MS. 1 μL of the extracted sample was injected in a split ratio 50:1 at 300°C. The initial temperature of the primary oven (80°C) was held for 2 min and then increased at 2°C min^{-1} to 210°C, followed by 1.5 °C min^{-1} to 325°C. The initial temperature of the secondary oven (120°C) was held for 2 min and then increased at 3°C min^{-1} to 200°C, followed by 2°C min^{-1} to 300°C and a final increase of 1°C min^{-1} to 330°C to ensure all species passed through the column. The transfer line temperature was 330°C and the ion source temperature was 280°C. Helium (99.999%) was used as the carrier gas at a constant flow rate of 1 mL min^{-1} . Further details of the instrumentation and data processing methods are given by Alam and Harrison (2016) and Alam et al. (2016a).

2.4 Qualitative and Quantitative Analysis

Standards used in these experiments included 26 n-alkanes (C_{11} to C_{36}), EPA's 16 priority pollutant PAHs, 4 hopanes (17 α (H),21 β (H)-22R-homohopane, 17 α (H),21 β (H)-hopane, 17b(H),21a(H)-30-

155 norhopane and 17 α (H)-22,29,30-trisnorhopane, 7 decalins and tetralines (cis/trans-decalin, tetralin, 5-
156 methyltetraline, 2,2,5,7-tetramethyltetraline, 2,5,8-trimethyltetraline and 1,4-dimethyltetraline), 4
157 alkyl-naphthalenes (1-methyl-naphthalene, 1-ethyl-naphthalene, 1-n-propyl-naphthalene and 1-n-
158 hexyl-naphthalene), 13 alkyl-cyclohexanes (n-heptyl-cyclohexane to n-nonadecyl-cyclohexane), 5
159 alkyl-benzenes (n-butyl-benzene, n-hexyl-benzene, n-octyl-benzene, n-decyl-benzene and n-dodecyl-
160 benzene) (Sigma-Aldrich, UK, purity >99.2%), 11 n-aldehydes (C₈ to C₁₃) (Sigma-Aldrich, UK, purity
161 $\geq 95.0\%$), C₁₄ to C₁₈ (Tokyo Chemical Industry UK Ltd, purity >95.0%); and 11 2-ketones, C₈ to C₁₃
162 and C₁₅ to C₁₈ (Sigma-Aldrich, UK, purity $\geq 98.0\%$) and C₁₄ (Tokyo Chemical Industry UK Ltd, purity
163 97.0%), 4 n-alcohols (2-decanol, 2-dodecanol, 2-hexadecanol and 2-nonadecanol) (Sigma-Aldrich, UK,
164 purity 99.0%) and 1-pentadecanol (Sigma-Aldrich, UK, purity 99.0%).

165

166 Compound identification was based on the GC \times GC-TOFMS spectral library, NIST mass spectral
167 library and on co-injection with authentic standards. Compounds within the homologous series for
168 which standards were not available were identified by comparing the retention time interval between
169 homologues, and by comparison of mass spectra with the standards for similar compounds within the
170 series, by comparison to the NIST mass spectral library, and by the analysis of fragmentation patterns.
171 The quantification for identified compounds was performed by the linear regression method using the
172 seven-point calibration curves (0.05, 0.10, 0.25, 0.50, 1.00, 2.00, 3.00 ng μL^{-1}) established between the
173 authentic standards/internal standard concentration ratios and the corresponding peak area ratios. The
174 calibration curves for all target compounds were highly linear ($r^2 > 0.98$, from 0.978 to 0.998),
175 demonstrating the consistency and reproducibility of this method. Limits of detection for individual
176 compounds were typically in the range 0.001–0.08 ng m^{-3} . The identified compounds which have no
177 commercial authentic standards were quantified using the calibration curves for similar structure
178 compounds or isomeric compounds. This applicability of quantification of individual compounds using

isomers of the same compound functionality (which have authentic standards) has been discussed elsewhere and has a reported uncertainty of 24% (Alam et al., 2018).

The branched alkanes, alkyl-benzenes, alkyl-decalins, alkyl-phenanthrene and anthracene (alkyl-Phe and Ant), alkyl-naphthalene (alkyl-Nap) and alkyl-benzaldehyde were identified in the samples with the graphics method of the GC Image v2.5 (Zoex Corporation, Houston, US), and the detailed descriptions are given elsewhere (Alam et al., 2018). Briefly, the structurally similar compounds (similar physico-chemical properties) were identified as a group via drawing a polygon around a section of the chromatogram with the polygon selection tool. All compounds included in the polygon belong to a special compound class and the total concentrations were calculated via a calibration curve of the adjacent compounds and internal standards (IS).

Field and laboratory blanks were routinely analysed to evaluate analytical bias and precision. Blank levels of individual analytes were normally very low and, in most cases, not detectable. The major contaminants observed were very minor amounts of n-alkanes ranging from C₁₁ to C₂₁, with no carbon number predominance and maximum at C₁₈; PAH were not detectable. The major proportion of the contaminants could be distinguished by their low concentrations and distribution fingerprints (especially the n-alkanes). These contaminants did not interfere with the recognition or quantification of the compounds of interest. Recovery efficiencies were determined by analysing the blank samples spiked with standard compounds. Mean recoveries ranged between 82 and 98%. All quantities reported here have been corrected according to their recovery efficiencies. Analytical data from the GC×GC analysis were compared with a conventional GC-MS analysis for levoglucosan and 13 PAH. The results from two analytical instruments were compared, and the correlations (r^2) between them were in the range of 0.5 to 0.8 with 10 mean concentrations of individual compounds from each technique within 20% of one

another, 2 within 20-30% and the remainder (2) within 30-40% of one another. The largest outlier was levoglucosan, which was underestimated, probably since it decomposed due to a lack of the usual derivatisation.

3. RESULTS AND DISCUSSION

3.1 General Aerosol Characteristics

Thirty-three samples were separated into non-haze (13) and haze (20) days (the latter with $PM_{2.5}$ exceeding $75 \mu g m^{-3}$ for 24 h average) according to the National Ambient Air Quality Standards of China (NAAQS) released in 2012 by the Ministry of Environmental Protection (MEP) of the People's Republic of China. The concentrations of $PM_{2.5}$, black carbon (BC), organic carbon (OC), element carbon (EC), gaseous pollutants (SO_2 , NO, NO_2 , NO_x , and CO) and meteorological parameters (wind speed (WS), wind direction (WD) and relative humidity (RH)) were simultaneously determined during the field campaigns and appear in Table S1.

The average daily $PM_{2.5}$ mass was $99 \mu g m^{-3}$, and haze days (average $141 \mu g m^{-3}$) were four times higher than that of non-haze days ($35.3 \mu g m^{-3}$). The wind and temperature during the haze and non-haze days were 0.94 and 1.44 m/s, 6.07 and 4.0°C, respectively. However, the relative humidity during haze episodes (56.3%) was slightly higher than the non-haze periods (39.8%). The concentrations of gaseous pollutants SO_x , NO_x , and CO were simultaneously elevated with the increase of $PM_{2.5}$ concentrations, whereas the O_3 concentration presented an opposite trend to $PM_{2.5}$ concentrations (Lyu et al., 2019). The average concentration of organic matter (OM) was estimated as $30.2 \mu g m^{-3}$ using the OC concentration ($18.9 \mu g m^{-3}$) and a multiplying factor of 1.6 for aged aerosols (Turpin and Lim, 2001). The OM concentration was $40.0 \mu g m^{-3}$ and $15.0 \mu g m^{-3}$ on haze and non-haze days respectively.

227 **3.2 The Major Classes of Organic Compounds in PM_{2.5}**

228 More than 6000 peaks were found in the 2D chromatogram image of each sample by the data processing
229 software (GC Image v2.5). Over 300 polar and non-polar organic compounds (POCs and N-POCs) were
230 identified and quantified in the PM_{2.5} samples, and these compounds are grouped into more than twenty
231 classes, including normal and branched alkanes, n-alkenes, aliphatic carbonyl compounds (1-alkanals, n-
232 alkan-2-ones and n-alkan-3-ones), n-alkanoic acids, n-alkanols, PAHs, oxygenated PAHs (OPAHs),
233 alkylated-PAHs, hopanes, alkyls-benzenes, alkyl-cyclohexanes, pyridines, quinolines, furanones, and
234 biomarkers (levoglucosan, cedrol, phytane, pristane, supraene and phytone). The details of aliphatic
235 hydrocarbon measurements (including n-alkanes, n-alkenes) and carbonyl compounds (including n-
236 alkanals, n-alkan-2-ones, n-alkan-3-ones, furanones and phytone) have been reported in previous articles
237 (Lyu et al. 2018a,b). The total concentrations of identified organic compounds ranged from 0.94 to 5.14
238 $\mu\text{g m}^{-3}$ with the average of $2.84 \pm 1.19 \mu\text{g m}^{-3}$, accounting for 9.40 % of OM. The concentrations of
239 identified individual organic compounds are summarized in Table S2, and the percentage of each group
240 in the total identified organic compounds is in Figure 1. The n-alkanes (16%) make the greatest
241 contribution to the total mass of identified organic compounds, followed by levoglucosan (13%),
242 branched-alkanes (13%), PAHs (10%), n-alkenes (7%) and alkyl-benzenes (7%). These six groups
243 account for 66% of total identified organic compounds by mass, and a total concentration of $1.41 \mu\text{g m}^{-3}$,
244 accounting for 1.42% of the particle mass. In a study in Nanjing, Haque et al. (2019) reported the most
245 abundant classes of organic compounds to be n-alkanes (205 ng m^{-3}), followed by fatty acids (76.3 ng m^{-3}),
246 PAHs (64.3 ng m^{-3}), anhydrosugars (levoglucosan, galactosan and mannosan, 56.3 ng m^{-3}), fatty
247 alcohols (40.5 ng m^{-3}) and phthalate esters (15.2 ng m^{-3}).

248

249 **3.3 The Characteristics of Organic Compound Groups on Non-haze and Haze Days**

250 The average total concentration of identified groups was calculated for the non-haze (13 days) and haze
251 periods (20 days). The comparisons of two periods (non-haze and haze days) are shown in Figure 2, and
252 the detailed concentrations of each group are shown in the Table S3. The concentrations of most organic
253 compound groups on the haze days were higher than non-haze days, especially for the n-alkanols and n-
254 Cn-cyclohexanes. The alkyl-benzenes, alkyl-benzaldehydes, monoaromatic compounds and quinoline
255 have approximately similar concentrations on the non-haze and haze days.

256

257 As many compound groups have not been reported in previous studies, and complete data on the relative
258 abundance of these compounds in various source emissions are not available at present, it is not yet
259 possible to calculate source contributions to ambient organic compound concentrations via molecular
260 marker or mathematical modelling methods. However, several important consistency checks on the
261 potential source can be performed. In the sections that follow, the literature on the origin of each of these
262 compound classes is reviewed briefly and the measured compound concentrations are described. Table
263 1 shows the comparison of identified organic compounds between the present and previous studies in
264 Beijing. In many, but not all cases, concentrations are comparable.

265

266 **3.3.1 n-Alkanoic acids, n-alkanols and carbonyl compounds**

267 The n-alkanoic acids with carbon numbers from C₆ to C₁₀ were identified in the PM_{2.5}. Higher molecular
268 weight alkanoic acids generated from the biomass burning (Simoneit and Mazurek, 1982) were not
269 identified from the samples probably due to low volatility in the G.C. The n-alkanoic acids were
270 observed at a similar magnitude to a previous study in Beijing (Zhou et al., 2009) (Table 1).

271

272 Previous studies have found that the n-alkanoic acid homologues were significantly impacted by cooking

emissions in Beijing and showed higher concentrations on non-haze days and a similar distribution pattern in all seasons (Huang et al., 2006; He et al., 2006b; Sun et al. 2013). Consistent results for acids were observed in this study, and the Σ n-alkanoic acids had an average concentration on the non-haze days with an average concentration of 36.4 ng m^{-3} , higher than 24.6 ng m^{-3} on haze days, strongly implying a dominant contribution from cooking emissions as opposed to secondary formation.

In the present study, 1-alkanols with even-carbon numbers from C_{12} to C_{20} were identified in the $\text{PM}_{2.5}$, with a quite similar molecular distribution to that of diesel engine exhaust samples (Alam et al., 2016b). In addition, other primary emission sources may make a potential contribution to these compounds, including from biomass burning (Zhang et al., 2007). The average Σ n-alkanols concentration was 38.5 ng m^{-3} , and Σ n-alkanols had higher concentrations on the haze days (59.8 ng m^{-3}), approximately eight times greater than 8.39 ng m^{-3} on non-haze days. The above results suggest that n-alkanol formation is more efficient on haze days, even though vehicular emissions appear to be another important source.

Aliphatic carbonyl compounds including n-alkanals, n-alkan-2-ones and n-alkan-3-ones, have been described in detail by Lyu et al. (2019). Briefly, the daily sum of aliphatic carbonyls (ΣAC), ranged from 8.87 to 164 ng m^{-3} , accounting for 0.02 – 0.46% of OM. The average ΣAC was 75.8 ng m^{-3} during all haze days, approximately double the 39.5 ng m^{-3} of the non-haze period. Lyu et al. (2019) showed that the n-alkanals were mainly originated from vehicle exhaust or formed from OH oxidation of n-alkanes, while the n-alkanones were probably emitted mainly by coal combustion.

3.3.2 Nitrogen-containing organic compounds (N-CC)

Nitrogen-containing (N-containing) organic compounds have been reported in many previous studies, and the important sources of N-containing compounds are coal combustion, biomass burning, vehicular

297 exhaust and atmospheric photochemical reactions (Rogge et al., 1994; Rogge et al., 1993b; Schauer et
298 al., 1996; Zhang et al., 2002; Zhang et al. 2002; Fan et al. 2018). N-containing compounds were
299 identified in the samples, including heterocyclic compounds (alkyl-pyridines, alkyl-quinolines) and other
300 N-containing compounds (nitro, amine compounds). The average Σ alkyl-pyridines, Σ alkyl-quinolines
301 and Σ other N-containing compounds were 17.4 ± 7.58 , 16.6 ± 15.0 and 30.0 ± 23.1 ng m⁻³, respectively,
302 and the average total concentrations of N-containing compounds was 64.0 ng m⁻³, accounting for
303 approximately 0.2% of the OM.

304

305 The quinolines have been proposed for use as tracers of vehicular exhaust (Rogge et al., 1993a) and crude
306 oils and shale oil combustions (Schmitter et al., 1983; Simoneit et al., 1971), while the straight chain
307 alkyl-pyridines (n-Cn-pyridine) are related to petrochemical industries (Botalova et al., 2009) and
308 secondary formation from pyrolysis of proteins and amino acids under a high temperature (Chiavari and
309 Galletti, 1992; Hendricker and Voorhees, 1998; Kögel-Knabner, 1997). This study found that both
310 quinolines and alkyl-pyridines showed similar concentrations on the non-haze and haze days, 16.8 ± 16.5
311 ng m⁻³ (non-haze) and 16.5 ± 14.4 ng m⁻³ (haze days) and 12.0 ± 6.02 ng m⁻³ (non-haze days) and $15.3 \pm$
312 8.36 ng m⁻³ (haze days) respectively. Amino compounds can originate from biomass burning and coal
313 combustion, and are abundant in winter fine particulate matter samples compared to summer (Zhang et
314 al., 2002; Akyiiz 2008). In the present study, the average Σ other N-containing compounds was $34.2 \pm$
315 24.6 ng m⁻³ on the haze days, somewhat higher than 22.6 ± 19.4 ng m⁻³ on non-haze days.

316

317 The similar concentrations on the non-haze and haze days suggests that N-containing organic compounds
318 mainly originated from primary sources and subject to degradation during the haze formation process.

319

320 Tracers of tobacco smoke, benzoquinoline and isoquinoline have previously been determined in the PM

321 collected in Beijing, with concentrations of 3.10 and 0.22 ng m⁻³ respectively (Zhou et al., 2009). These
322 two compounds were also identified in the present study, with 4.40 and 0.80 ng m⁻³, respectively.
323 Phthalimide was identified in the PM at 0.91 ng m⁻³, and was considered to be derived from cyclization
324 and aromatization reactions of proteins or from intermediates in the transformation of carboxyl
325 ammonium salts to nitriles by Zhao et al. (2009).

326

327 3.3.3 Esters

328 Phthalate esters are organic chemicals that are commonly used in a variety of consumer products and in
329 various industrial and medical applications, and are predominantly used as plasticizers to improve the
330 flexibility of polyvinyl chloride (PVC) resins and other polymers. Table 1 shows a comparison of
331 phthalate esters (DBP, DEP, DEHP) between the present and previous studies in the winter in Beijing; it
332 seems that the concentrations of some phthalate esters have significantly decreased from earlier studies
333 (Wang et al., 2006; Zhou et al., 2009). The present study found that diisodecyl phthalates, DBP and
334 DEHP were abundant compounds in the ester group with 49.7 ± 43.2 , 16.9 ± 15.5 and 16.0 ± 12.6 ng m⁻³,
335 respectively. The DBP, DEP and DEHP in Beijing were far lower than that in winter in Tianjin (Kong
336 et al., 2013) and another fifteen cities around China (Li and Wang, 2015; Wang and Kawamura, 2005;
337 Wang et al., 2006). In addition, the average \sum Ester was 117 ± 82.1 ng m⁻³, with 132 ± 87.1 and $89.4 \pm$
338 70.0 ng m⁻³ on haze and non-haze days, respectively. Since phthalates are not chemically bound to the
339 polymeric matrix, they can enter the environment by escaping from manufacturing processes and by
340 leaching or vaporising from final products (Staples et al., 1997).

341

342 3.3.4 PAHs, O-PAHs and alkylated-(PAHs & OPAHs)

343 In all, 23 PAHs (2-6 rings), 19 oxygenated PAHs (O-PAHs) and 14 alkylated-(PAHs & OPAHs) were
344 determined in the PM_{2.5} samples. The average total polycyclic aromatic compounds (the sum of \sum PAHs,

345 Σ O-PAHs, Σ alkylated-(PAHs & OPAHs), alkyl-PHE and ANT and alkyl-NAP) was 569 ng m⁻³,
346 accounting for 1.88 % of OM.

347
348 The distribution of PAHs is shown in Figure 3; the most abundant PAHs were BbF, followed by CHR,
349 FLT, BaA and PYR. In all samples, the Σ PAHs ranged from 46.7-727 ng m⁻³ with average 281 ± 176
350 ng m⁻³, accounting for 0.93 % of OM. In addition, the average Σ PAHs was 364 ng m⁻³ during haze days,
351 but only 159 ng m⁻³ on the non-haze days. It should be noted that retene was detected in most samples,
352 with an average concentration of 14.4 ± 17.5 ng m⁻³. It has been suggested that retene predominantly
353 originates from the combustion of conifer wood (Simoneit et al., 1991).

354
355 Nineteen oxygenated PAHs (O-PAHs) make up of a class of PAH derivatives that are present in the
356 atmosphere as a result of direct emission during combustion and secondary formation by homogeneous
357 and heterogeneous photo-oxidation processes (Keyte et al., 2013; Ringuet et al., 2012). They are also of
358 scientific interest because they are, typically, found in the secondary organic aerosol (SOA) formed by
359 photo-oxidation of PAH (Shakya and Griffin, 2010). In urban samples, polycyclic aromatic ketones
360 (PAK), polycyclic aromatic quinones (PAQ) and polycyclic aromatic furanones (PAF) are typical groups
361 of compounds (Lin et al., 2015). The average total concentrations of O-PAH measured in this study
362 (Figure 4) was 67.9 ng m⁻³. The polycyclic aromatic ketones 4,5-pyrenequinone (4,5-PyrQ) (8.75 ng m⁻³)
363 and 1,6-pyrenequinone (1,6-PyrQ) (7.38 ng m⁻³) were the most abundant compounds during the
364 sampling campaign. Four O-PAHs have been identified previously at the PKU site in the 2012 heating
365 season in Beijing (Table 1); it is notable that the concentration of AQ was up to 108 ng m⁻³,
366 approximately 20 times that in the present study (5.12 ng m⁻³). As O-PAHs can be formed during
367 sampling, it is necessary to be very careful in reconciling their presence with specific sources (Pitts et al.,
368 1980). The average Σ O-PAHs was 86.5 ng m⁻³ during haze days, but 39.7 ng m⁻³ on the non-haze days.

369 The ratio of quinone: parent PAH has been used to assess the air mass age (Alam et al., 2014; Harrison
370 et al., 2016). The average ratios of phenanthraquinone to phenanthrene (PQ:PHE), anthraquinone to
371 anthracene (AQ:ANT) and benzo(a)anthracene-7,12-quinone to benzo(a)anthracene (BaAQ:BaA) were
372 0.37, 1.27, 0.32, respectively, with PQ:PHE, AQ:ANT and BaAQ:BaA ratios of 0.25, 0.88 and 0.26 on
373 the haze days, which were lower than 0.55, 1.92, 0.40 on non-haze days. The BaAQ:BaA ratios were
374 lower than earlier published data of 1.28 measured in Beijing (Li et al., 2019), 1.40 in Xian (Wang et al.,
375 2016) and 0.54 in Beijing-Tianjing (Wang, 2010), but higher than the 0.08 measured in Guangzhou (Wei
376 et al., 2012) and 0.09 in Zhuanghu (Ding et al., 2012). Shen et al. (2011) reported that the BaAQ:BaA
377 ratio was 0.03 for coal combustion, 0.16 for crop residue burning (Shen et al., 2012a) and 6.6 from
378 biomass pellet burning (Shen et al., 2012b). The low ratios of O-PAHs/PAHs in our data probably
379 indicated that the particulate matter mainly originated from coal combustion and biomass burning.
380 However, the lower ratios on haze days than non-haze days may imply continued oxidation of the O-
381 PAH to products which were not analysed. Li et al. (2019) also reported that ratios of Σ OPAH to Σ PAH
382 were very similar during haze and clean air periods, which provides support for this conclusion.

383

384 **3.3.5 Molecular markers**

385 The hopanes are compounds present in crude oil as a result of the decomposition of sterols and other
386 biomass and are not by-products of combustion (Simoneit, 1985). They are very stable and have been
387 proposed for use as tracers for atmospheric particles from fossil fuel combustion, such as motor vehicle
388 exhaust (Simoneit, 1985) and coal combustion (Oros and Simoneit, 2000). The hopanes are widely used
389 as tracers of traffic emission due to vehicle emissions having high loadings of hopanes (Cass, 1998). The
390 comparison of hopanes between this study and previous studies in the winter or heating season of Beijing
391 are shown in Table 1. Hopanes were extensively present in Beijing PM_{2.5} samples, and their carbon
392 numbers ranged from C₂₇ to C₃₂, but not C₂₈ (Table 2). The average concentration of hopanes in Beijing

393 was $32.7 \pm 24.7 \text{ ng m}^{-3}$, with $15.2 \pm 10.7 \text{ ng m}^{-3}$ and $44.6 \pm 24.6 \text{ ng m}^{-3}$ on non-haze and haze days,
394 respectively. Previous studies have found that C_{29} (17a(H), 21h(H)-norhopane) was dominant in the
395 hopane series and consistent with that from coal combustion (He et al., 2006a), while C_{30} (17 β (H)21 α (H)-
396 hopane and 17a(H), 21 β (H)-hopane) was similar to C_{29} in the winter time in Beijing and attributed to
397 gasoline and diesel exhaust (Simoneit, 1985).

398

399 Levoglucosan and methoxyphenols from pyrolysis of cellulose and lignin are usually used as unique
400 tracers for biomass burning in source apportionment models (Schauer and Cass, 2000). Levoglucosan
401 (1,6-anhydro- β -D-glucopyranose) has been for a long time employed as the specific molecular marker
402 for long-range transport of biomass burning aerosol, based on its high emission factors and assumed
403 chemical stability (Fraser and Lakshmanan, 2000; Simoneit et al., 2000). It is a highly abundant
404 compound and the concentrations in winter in Beijing have a significant fluctuation (Table 1). The
405 average Σ levoglucosan was $355 \pm 232 \text{ ng m}^{-3}$ during the entire sampling period, and $417 \pm 223 \text{ ng m}^{-3}$
406 in haze episodes, approximately twofold that of the non-haze days, $238 \pm 193 \text{ ng m}^{-3}$, indicating a
407 significant impact of biomass burning upon wintertime aerosols in Beijing.

408

409 Methoxyphenols are usually also considered as tracers for wood burning (Simpson et al., 2005; Yee et
410 al., 2013) with the average Σ Methoxyphenols $7.29 \pm 7.11 \text{ ng m}^{-3}$, and the haze days ($9.03 \pm 7.93 \text{ ng m}^{-3}$)
411 twofold greater than non-haze days ($4.74 \pm 4.95 \text{ ng m}^{-3}$) during the campaigns. In Beijing and its
412 surrounding areas, harvest occurs in late September to October for corn, and biomass fuels are used for
413 cooking and heating purpose in the winter. However, the methoxyphenols are abundant components in
414 the smoke from broad-leaf tree and shrub burning (Wang et al., 2009), and have been identified in all
415 coal smoke (Simoneit, 2002a), so cannot be used as source-specific markers for biomass burning.

416

417 Phenolic compounds from the thermal degradation of lignin have been proposed as potentially useful
418 tracers for wood smoke, and many of them are emitted in relatively high quantities and are specific to
419 wood combustion sources (Simoneit, 2002b; Simoneit et al., 2004). Another important source of phenolic
420 compounds is oxidation of monoaromatic compounds and PAHs (Pan and Wang, 2014). Phenols and
421 naphthalenol were identified in the PM_{2.5}, with the average Σ phenolic compounds $21.6 \pm 17.0 \text{ ng m}^{-3}$,
422 with $14.0 \pm 13.2 \text{ ng m}^{-3}$ and $25.9 \pm 17.9 \text{ ng m}^{-3}$ on the non-haze and haze days, respectively. However, it
423 is notable that the concentrations of naphthalenol identified in the present study were far lower than that
424 of previous studies (Table 1).

425

426 Pristane (Pr) and phytane (Ph) have been found in the exhaust of petrol and diesel engines and in
427 lubricating oil, indicating their origin from petroleum (Simoneit, 1984). Since their presence is ubiquitous
428 in vehicle exhausts and negligible in contemporary biogenic sources in urban environments, they can be
429 used as petroleum tracers for airborne particulate matter. The mean values of Pr and Ph in our samples
430 are 2.24 and 1.94 ng m^{-3} , respectively. Biogenic inputs are often characterised by a predominance of the
431 odd carbon alkanes and Pr. Since Ph is rarely found in biological material, most biological hydrocarbons
432 have a Pr/Ph ratio far higher than 1.0 (Oliveira et al., 2007), but values approaching unity indicate a
433 hydrocarbon signature derived from petrochemical use. The average Pr/Ph ratios were 1.15 for PM_{2.5}
434 samples, and this finding is quite similar to the results from the southern Chinese city of Guangzhou, 1.1-
435 1.8 (Bi et al., 2002), but almost four times greater than Beijing summer samples (0.3) (Simoneit et al.,
436 1991). The high Pr/Ph indicated that the hydrocarbons in urban aerosol derive mainly from petroleum
437 residues probably deriving from vehicular emissions in Beijing.

438

439 **3.4 The Molecular Distributions of Aliphatic Hydrocarbons**

440 Figure 4 shows the molecular distributions of aliphatic hydrocarbons on non-haze and haze days. The

441 details on the n-alkanes are given by Lyu et al. (2019). Briefly, the Σ n-alkanes (C_{10} - C_{36}) ranged from
442 42.4 to 1241 ng m^{-3} with an average $450 \pm 316 \text{ ng m}^{-3}$, and the average Σ n-alkanes was 577 ng m^{-3} during
443 haze episodes, more than twice that of the non-haze period (264 ng m^{-3}). The n-alkanes (C_{20} - C_{31}) were
444 the most abundant homologues (Figure 4), accounting for approximately 83% of the Σ n-alkanes.

445

446 The total concentrations of branched alkanes (C_{12} - C_{36}) ranged from 125-647 ng m^{-3} with the average 356
447 $\pm 173 \text{ ng m}^{-3}$ during the sampling period. The average branched alkanes concentration was $440 \pm 144 \text{ ng}$
448 m^{-3} during all haze episodes, which was higher than $234 \pm 138 \text{ ng m}^{-3}$ on the non-haze days. The most
449 abundant branched alkanes were observed at C_{22} , with the average concentration of 29.2 ng m^{-3} , and the
450 greatest abundance of branched alkanes groups was observed within the carbon atom range of C_{20} - C_{30} ,
451 accounting for 67.7% of Σ branched alkanes. The branched alkanes have lower concentrations than n-
452 alkanes when the carbon number is $>C_{20}$ on haze and non-haze days, while showing higher
453 concentrations than n-alkanes when the carbon number is lower than C_{19} .

454

455 It is difficult to identify the potential sources of branched alkanes from the literature, although Alam et
456 al. (2016b) reported that branched alkanes (C_{11} - C_{33}) were an abundant compound group in diesel exhaust.
457 The increase of high molecular weight branched alkanes (C_{20} - C_{30}) from non-haze days to haze days is
458 consistent with a primary emission source, probably linked to coal combustion or vehicular emissions.
459 The fact that both n-alkanes and branched alkanes increase quite similarly between non-haze and haze
460 conditions is consistent with them arising from the same source(s), or sources with highly correlated
461 emissions.

462

463 Other groups of aliphatic and alicyclic compounds identified in the $\text{PM}_{2.5}$, include alkyl-decalins, alkyl-
464 pyridines, alkyl-furanones, alkyl-cyclohexanes and alkyl-benzenes. Figure 5 shows the molecular

distributions of these series of compounds. Engine studies (Alam et al., 2016b) have also found that compounds observed in vehicle exhaust beside n-alkanes and PAHs, include straight and branched cyclohexanes (C₁₁-C₂₅), various cyclic aromatics, alkyl-decalins and alkyl-benzenes. The particle-bound n-C_n-cyclohexanes with carbon numbers from C₁₂ to C₂₆ were identified in diesel exhaust (Alam et al., 2016b) with a dominant range C₁₈-C₂₅, and the total (particle + gas) concentration of n-C_n-cyclohexanes was 2.05 µg m⁻³. The n-C_n-cyclohexanes (C₂₀-C₃₀) were identified at the IAP site with average \sum n-C_n-cyclohexane 39.4 ± 37.1 ng m⁻³. The most abundant range was observed at C₂₂-C₂₇, highly consistent with the engine study, implying a significant contribution from vehicle emissions. In addition, the average \sum n-C_n-cyclohexane (C₂₀-C₃₀) was 53.3 ± 39.3 ng m⁻³ during haze episodes, approximately five times higher than 10.8 ± 8.22 ng m⁻³ in the non-haze period, a larger ratio than for other primary emissions. The alkyl-decalins and tetralin are products obtained by hydrogenation of naphthalene and its derivatives during the refining process and have been identified in vehicle exhaust (Afzal et al., 2008; Alam et al., 2016b; Ogawa et al., 2007). The average \sum alkyl-decalins was 110 ng m⁻³, with 85.4 ± 65.5 and 126 ± 110 ng m⁻³ on non-haze and haze days respectively. The \sum n-C_n-benzene (C₁₆-C₂₅) identified in the samples ranged from 7.71 to 410 ng m⁻³ with an average of 56.6 ± 73.0 ng m⁻³. The average \sum n-C_n-benzene (C₁₆-C₂₅) was 77.2 ± 88.2 ng m⁻³ during haze episodes, approximately four times the 23.3 ± 15.1 ng m⁻³ of the non-haze period. Other alkyl-benzenes (C₉-C₂₅) were also identified and have higher concentrations at C₁₂, especially for the non-haze days.

483

484 **3.5 Distribution of Compounds with respect to Volatility and Polarity, and the Estimation of** 485 **Unidentified Mass**

486 The method for characterising the volatility/polarity distribution of compounds is detailed in the
487 Supporting Information. Briefly, the chromatography image was separated into seven parts according to
488 the main chemical and physical properties of the organic compounds and the distribution of internal

standards (IS), and the detailed protocol is shown in Table S4. The diagram of the separated image with seven parts is shown in Figure 6a, and the concentrations measured in each part are shown in Figure 6 and Table 3. In the chromatogram (Figure 6), volatility decreases from left to right and polarity increases from bottom to top. Table 3 shows the estimated mass concentration of all components of the chromatogram, alongside the amount of mass not accounted for by the specific compounds reported in this paper.

495

For the non-haze days, the sum of identified organic compounds (IOC) with carbon numbers higher than C_6 was $1.84 \mu\text{g m}^{-3}$, accounting for 46.5 % of total organic compounds. The IOC of the haze days was almost two times that of non-haze periods, with an average of $3.42 \mu\text{g m}^{-3}$, accounting for 46.3% of total measured organic matter. In addition, the sum of unidentified compounds increased from $2.12 \mu\text{g m}^{-3}$ on non-haze days to $3.96 \mu\text{g m}^{-3}$ on haze days, accounting for 53.5 % and 53.7% of total measured organic matter, respectively. Hence there is no marked difference in the proportions of identified and unidentified compounds between haze and non-haze conditions.

503

For the non-haze days, Section 1 of the chromatogram has the highest concentration of 802 ng m^{-3} , followed by Section 7 (792 ng m^{-3}), accounting for 20.3 % and 20.0 % of the total organic compounds respectively, implying that both low molecular weight (LMW) hydrocarbons (Section 1) and high molecular weight (HMW) PAHs (Section 7, 3~6 rings) and compounds of similar volatility/polarity were the main organic components of atmospheric particulate matter measureable by the GCxGC separation technique. The PAHs are important organic compounds appearing in Sections 6 + 7, accounting for 32.3% of total measured organic compounds during the non-haze days. Sections 2, 3 and 4 showed relatively low concentrations, and medium molecular weight hydrocarbons in the range of $C_{23}\sim C_{27}$ (Section 3) were the more abundant aliphatic hydrocarbons relative to Section 2 ($C_{17}\sim C_{23}$) and Section 4 ($>C_{27}$), probably

513 caused by primary emissions from vehicular and coal combustion (Cao et al., 2018). Section 5 contains
514 oxidized monoaromatic compounds, and the concentrations were higher than Section 6 (mainly
515 containing naphthalene derivatives) and lower than Section 1, probably mainly arising from vehicular
516 emissions or oxidized from the monoaromatic precursors (Section 1) (Schwantes et al., 2017).

517

518 The polarity distribution characteristics of atmospheric organic compounds on the non-haze days were
519 also studied. For the volatile areas, low polarity compounds (Section 1) have a lower concentration than
520 polar compounds (Sections 5 + 6) during the non-haze days. On the contrary, for the semi-and non-
521 volatile area, the sum of low polar compounds (Sections 2 + 3 + 4) have higher concentrations than polar
522 organic compounds (Section 7).

523

524 The concentrations in all sections increased from non-haze to haze days, and the main difference between
525 haze and non-haze days attaches to Sections 5, 6 and 7 (Figure 6b), indicating a more polar aerosol during
526 periods of haze. Section 6 has the highest concentrations on the haze days (1556 ng m^{-3}), increased more
527 than three times on the haze days in contrast to non-haze days (485 ng m^{-3}), followed by Section 7 (1337
528 ng m^{-3}) and Section 5 (1309 ng m^{-3}), indicating that the oxidized monoaromatics, naphthalene derivatives
529 and oxidized HMW PAHs were the main identified components of the atmospheric particulate matter
530 during the haze days. The concentrations were compared among the seven sections, and the highest
531 concentrations of Section 6 were probably contributed by the degradation of HMW PAHs (from Section
532 7). For the oxidized monoaromatic compounds (Section 5), the degradation of naphthalene derivatives
533 was probably a major contributor, but not compounds oxidized from Section 1. The concentrations of
534 Section 3 were also observed to increase from non-haze days (573 ng m^{-3}) to haze days (1060 ng m^{-3}),
535 indicating that accumulation has an obvious effect on the stable compounds with carbon number between
536 C_{23} to C_{27} during haze formation under low wind speed (Table S1).

537 **3.6 Elevation of Primary and Secondary Constituents during Haze Events**

538 By definition, concentrations of PM_{2.5} are elevated during haze events, but the question arises as to
539 whether primary or secondary organic compounds make a larger contribution to the rise in concentrations.
540 Constituents that are expected to be primary are typically elevated in mean concentration by a factor of
541 around two (Table S3). Examples are n-alkanes (ratio of haze : non-haze of 2.2), levoglucosan (1.8) and
542 hopanes (2.9). This is consistent with the ratios for primary gaseous emissions, including SO₂ (ratio of
543 2.6), CO (2.5) and NO_x (2.2) (Table S1). Surprisingly, however, both BC (ratio of 3.8) and EC (3.4)
544 (Table S1) are primary constituents with a large haze:non-haze ratio, comparable to that of PM_{2.5} mass
545 (4.0). Consequently the factors leading to an elevation of concentrations during the haze appear complex
546 and are likely to be resolved fully only by chemistry-transport models.

547

548 OC/EC ratios are used to estimate the relative contribution of primary and secondary sources; high
549 OC/EC ratios (> 2.0) have been observed for aerosols with significant SOA contributions in Beijing (Lv
550 et al., 2019; Ji et al., 2018). The OC/EC ratio in this study was 3.88 on average, suggesting a significant
551 contribution of SOA in Beijing aerosols, which is consistent with the results of Section 3.5. The aliphatic
552 carbonyls, which have both primary and secondary sources (Lyu et al., 2018a,b) range from ratios of 1.6
553 (n-alkanals) to 2.8 (n-alkan-2-ones). This result was consistent with Section 3.5; it was found that the
554 chromatogram Sections 2 and 3 which contained alkanals (C₁₅≤C_n≤C₂₅) and alkanones (C₁₅≤C_n≤C₂₅)
555 have slightly higher concentrations on haze days than non-haze days. However, the low ratio alkanal and
556 alkanone compounds are quite readily oxidised (Chacon-Madrid et al., 2010; Chacon-Madrid and
557 Donahue, 2011), and a low ratio may reflect a high degree of further processing to form more oxidised
558 species on the haze days compensating for enhanced formation.

559

560 There are no compounds in Table S3 certain to be exclusively secondary. However, the results in Figure

6 show an appreciable elevation in more polar compounds (upper part of the chromatogram) on haze days, suggestive of a greater relative abundance of more oxidised, possibly secondary compounds in the haze. The ratio of average PM_{2.5} mass between haze and non-haze days was 4.0, and organic carbon, 2.7 (Table S1). The ratio for organic matter would be greater than 2.7, due to a higher OM/OC ratio in secondary compounds. This is strongly suggestive of a greater contribution from an elevation in secondary than primary species concentrations during the haze events, and that much of the mass lies outside of the chromatogram due to the low volatility of the secondary species.

568
569

570 **4. CONCLUSIONS**

571 Over 300 polar and non-polar organic compounds were determined in the fine particle samples from
572 Beijing, and these compounds have been grouped into more than twenty classes, including normal and
573 branched alkanes, n-alkenes, aliphatic carbonyl compounds (1-alkanals, n-alkan-2-ones and n-alkan-3-
574 ones), n-alkanoic acids, n-alkanols, PAHs, oxygenated PAHs (O-PAHs), alkylated-(PAHs & OPAHs),
575 hopanes, n-C_n-benzene, alkyls-benzenes, n-C_n-cyclohexane, pyridines, quinolines, furanones, and
576 biomarkers (levoglucosan, cedrol, phytane, pristane, supraene and phytone). The total concentrations of
577 identified organic compounds ranged from 0.94 to 5.14 $\mu\text{g m}^{-3}$ with an average of $2.84 \pm 1.19 \mu\text{g m}^{-3}$,
578 accounting for 9.40 % of OM mass. The six groups which accounted for 66% of total identified organic
579 compound mass included n-alkanes, levoglucosan, branched-alkanes, PAHs, n-alkenes and alkyl-
580 benzenes, and these were significantly impacted by primary emission sources. In addition, the average
581 total polycyclic aromatic compounds (the sum of \sum PAHs, \sum O-PAHs, \sum alkylated-(PAHs & OPAHs),
582 alkyl-PHE and ANT and alkyl-NAP) was 560 ng m^{-3} , accounting for 1.88 % of OM. The comparisons
583 of identified groups between non-haze and haze periods showed that most organic compound groups
584 have a higher concentration on the haze days relative to the non-haze days. The average sum of the
585 identified compounds increased from 1.84 $\mu\text{g m}^{-3}$ to 3.42 $\mu\text{g m}^{-3}$ from non-haze days to haze days. A

unimodal molecular distribution of alkanes was observed in the range from C₈ to C₃₆, and these compounds make significant contributions to atmospheric organic compounds in the range of C₁₉-C₂₈, especially on the haze days. The unidentified compounds in the chromatogram were estimated, and the results show that the average sum of unidentified compounds increased from 2.12 µg m⁻³ on non-haze days to 3.96 µg m⁻³ on haze days, accounting approximately for 53.5 % and 53.7% of total organic compounds, respectively. Finally, the total mass concentrations of measured organic compounds (≥C₆) was 3.96 µg m⁻³ and 7.39 µg m⁻³ on the non-haze and haze days, accounting for 26.4% and 18.5% of OM mass, respectively on these days. The remaining mass is that which is not volatile under the conditions of the gas chromatography. The higher percentage of non-GC-volatile organic matter on haze days is indicative of a greater degree of oxidation of the organic aerosol, consistent with the difference in the chromatogram between haze and non-haze days. The greater contribution of secondary constituents during haze events has been reported previously by Huang et al. (2014) and Ma et al. (2017), but not the greater extent of oxidation of organic matter. In a modelling study, Li et al. (2017) found that during winter haze conditions in Beijing the majority of secondary PM_{2.5} had formed one or more days prior to arrival, hence explaining its highly oxidised condition.

601

602 DATA ACCESSIBILITY

603 Data supporting this publication are openly available from the UBIRA eData repository at
604 <https://doi.org/10.25500/edata.bham.00000303>.

605

606 AUTHOR CONTRIBUTIONS

607 The study was conceived by RMH and ZS and the fieldwork was organised and supervised by ZS and
608 PF. TV and DL undertook air sampling work and general data analyses for the campaign while RL
609 carried analytical work on the Beijing samples under the guidance of MSA and CS. XW contributed

610 analyses of data from London. RL produced the first draft of the manuscript with guidance from YF and
611 RMH and all authors contributed to the refinement of the submitted manuscript.

612

613 **ACKNOWLEDGEMENTS**

614 Primary collection of samples took place during the APHH project in which our work was funded by the
615 Natural Environment Research Council (NERC) (NE/N007190/1). The authors would also like to thank
616 the China Scholarship Council (CSC) for support to R.L.

617

618 **COMPETING INTERESTS**

619 The authors have no conflict of interest.

620

REFERENCES

- Afzal, A., Chelme-Ayala, P., El-Din, A. G., El-Din, M. G.: Automotive Wastes, *Water Environ., Res.*, 80, 1397-1415, 2008.
- Akyüz, M.: Simultaneous determination of aliphatic and aromatic amines in ambient air and airborne particulate matters by gas chromatography-mass spectrometry, *Atmos. Environ.*, 42, 3809-3819, 2008.
- Alam, M. S., Zeraati-Rezaei, S., Liang, Z., Stark, C., Xu, H., MacKenzie, A. R., Harrison, R. M.: Mapping and quantifying isomer sets of hydrocarbons ($\geq C_{12}$) in diesel exhaust, lubricating oil and diesel fuel samples using GC \times GC-ToF-MS, *Atmos. Meas. Tech.*, 11, 3047, 2018.
- Alam, M. S., Stark, C., Harrison, R. M.: Using variable ionisation energy time-of-flight mass spectrometry with comprehensive GC \times GC to identify isomeric species, *Anal. Chem.*, 88, 4211-4220, 2016a.
- Alam, M. S., Zeraati-Rezaei, S., Stark, C. P., Liang, Z., Xu, H., Harrison, R. M.: The characterisation of diesel exhaust particles - composition, size distribution and partitioning, *Faraday. Discuss.*, 189, 69-84, 2016b.
- Alam, M. S., Harrison R. M.: Recent advances in the application of 2-dimensional gas chromatography with soft and hard ionisation time-of-flight mass spectrometry in environmental analysis, *Chem. Sci.*, 7, 3968-3977, 2016.
- Alam, M., Delgado-Saborit, J. M., Stark, C., Harrison, R. M.: Investigating PAH relative reactivity using congener profiles, quinone measurements and back trajectories, *Atmos. Chem. Phys.*, 14, 2467-2477, 2014.
- Bi, X., Sheng, G., Peng, P.A., Zhang, Z., Fu, J.: Extractable organic matter in PM₁₀ from LiWan District of Guangzhou City, PR China, *Sci. Tot. Environ.*, 300, 213-228, 2002.
- Botalova, O., Schwarzbauer, J., Frauenrath, T., and Dsikowitzky, L.: Identification and chemical characterization of specific organic constituents of petrochemical effluents, *Water Res.*, 43, 3797-3812, 2009.
- Cao, R., Zhang, H., Geng, N., Fu, Q., Teng, M., Zou, L., Gao, Y., and Chen, J.: Diurnal variations of atmospheric polycyclic aromatic hydrocarbons (PAHs) during three sequent winter haze episodes in Beijing, China, *Sci. Tot. Environ.*, 625, 1486-1493, 2018.
- Cass, G. R.: Organic molecular tracers for particulate air pollution sources. *TrAC Trends Anal. Chem.*, 17, 356-366, 1998.
- Chacon-Madrid, H. J., and Donahue, N.: Fragmentation vs. functionalization: chemical aging and organic aerosol formation, *Atoms. Chem. Phys.*, 11, 10553-10563, 2011.
- Chacon-Madrid, H. J., Presto, A. A., and Donahue, N. M.: Functionalization vs. fragmentation: n-aldehyde oxidation mechanisms and secondary organic aerosol formation, *Phys. Chem. Chem. Phys.*, 12, 13975-13982, 2010.

669
 670 Chiavari, G., Galletti, G. C.: Pyrolysis - gas chromatography/mass spectrometry of amino acids,
 671 J.Anal.Appl. Pyrol., 24, 123-137, 1992.
 672
 673 Ding, J., Zhong, J., Yang, Y., Li, B., Shen, G., Su, Y., Chen, W., Shen, H., Wang, B., and Rong, W.:
 674 Occurrence and exposure to polycyclic aromatic hydrocarbons and their derivatives in a rural chinese
 675 home through biomass fuelled cooking, Environ. Pollut., 169, 160-166, 2012.
 676
 677 Fan, X., Wei, S., Zhu, M., Song, J., Peng, P. A.: Molecular characterization of primary humic-like
 678 substances in fine smoke particles by thermochemolysis–gas chromatography–mass spectrometry,
 679 Atmos. Environ., 180, 1-10, 2018.
 680
 681 Fraser, M. P., Lakshmanan, K.: Using levoglucosan as a molecular marker for the long-range transport
 682 of biomass combustion aerosols, Environ. Sci. Technol., 34, 4560-4564, 2000.
 683
 684 Gao, Y., Guo, X., Ji, H., Li, C., Ding, H., Briki, M., Tang, L., Zhang, Y.: Potential threat of heavy
 685 metals and PAHs in PM2. 5 in different urban functional areas of Beijing, Atmos. Res., 178, 6-16,
 686 2016.
 687
 688 Guo, S., Hu, M., Guo, Q., Zhang, X., Schauer, J., Zhang, R.: Quantitative evaluation of emission
 689 controls on primary and secondary organic aerosol sources during Beijing 2008 Olympics, Atmos.
 690 Chem. Phys., 13, 8303-8314, 2013.
 691
 692 Hamilton, J., Webb, P., Lewis, A., Hopkins, J., Smith, S., Davy, P.: Partially oxidised organic
 693 components in urban aerosol using GCXGC-TOF/MS. Atmos. Chem. Phys., 4, 1279-1290, 2004.
 694
 695 Haque, M., Kawamura, K., Deshmukh, D. K., Fang, C., Song, W., Mengying, B., and Zhang, Y.-L.:
 696 Characterization of organic aerosols from a Chinese megacity during winter: predominance of fossil
 697 fuel combustion, Atmos. Chem. Phys., 19, 5147-5164, 2019.
 698
 699 Harrison, R. M., Alam, M.S., Dang, J., Ismail, I., Basahi, J., Alghamdi, M. A., Hassan, I., Khoder, M.:
 700 Relationship of polycyclic aromatic hydrocarbons with oxy (quinone) and nitro derivatives during air
 701 mass transport, Sci. Tot. Environ., 572, 1175-1183, 2016.
 702
 703 He, L.-Y., Hu, M., Huang, X.-F., Zhang, Y.-H., Tang, X.-Y.: Seasonal pollution characteristics of
 704 organic compounds in atmospheric fine particles in Beijing, Sci. Tot. Environ., 359, 167-176, 2006a.
 705
 706 He, L.-Y., Hu, M., Huang, X.-F., Zhang, Y.-H., Tang, X.-Y.: Seasonal pollution characteristics of
 707 organic compounds in atmospheric fine particles in Beijing, Sci. Tot. Environ., 359, 167-176, 2006b.
 708
 709 Hendricker, A. D., Voorhees, K. J.: Amino acid and oligopeptide analysis using Curie-point pyrolysis
 710 mass spectrometry with in-situ thermal hydrolysis and methylation: mechanistic considerations, J.
 711 Anal. Appl. Pyrol., 48, 17-33, 1998.
 712
 713 Huang, R.-J., Zhang Y., Bozzetti, C., Ho, F.-H., Cao, J.-J., Han, Y., Daellenbach, K. R., Slowik, J. G.,
 714 Platt, S. M., Canonaco, F., Zotter, P., Wolf, R., Pieber, S. M., Brun, E. A., Crippa, M., Ciarelli, G.,
 715 Piazzalunga, A., Schwikowski, M., Abbaszade, G., Schnelle-Kreis, J., Zimmermann, R., An, Z., Szidat,

S., Baltensperger, U., El Haddad, I., Prevot, A. S. H.: High secondary aerosol contribution to particulate pollution during haze events in China, *Nature* 514, 218-222, 2014.

Huang, X.-F., He, L.-Y., Hu, M., Zhang, Y.-H.: Annual variation of particulate organic compounds in PM_{2.5} in the urban atmosphere of Beijing, *Atmos. Environ.*, 40, 2449-2458, 2006.

Keyte, I. J., Harrison, R. M., Lammel, G.: Chemical reactivity and long-range transport potential of polycyclic aromatic hydrocarbons—a review, *Chem. Soc.Rev.*, 42, 9333-9391, 2013.

Ji, D., Yan, Y., Wang, Z., He, J., Liu, B., Sun, Y., Gao, M., Li, Y., Cao, W., Cui, Y., Hu, B., Xin, J., Wang, L., Liu, Z., Tang, G., and Wang, Y.: Two-year continuous measurements of carbonaceous aerosols in urban Beijing, China: Temporal variations, characteristics and source analyses, *Chemosphere* 200, 191-200, 2018.

Kögel-Knabner, I.: ¹³C and ¹⁵N NMR spectroscopy as a tool in soil organic matter studies, *Geoderma* 80, 243-270, 1997.

Kong, S., Ji, Y., Liu, L., Chen, L., Zhao, X., Wang, J., Bai, Z., Sun, Z.: Spatial and temporal variation of phthalic acid esters (PAEs) in atmospheric PM₁₀ and PM_{2.5} and the influence of ambient temperature in Tianjin, China, *Atmos. Environ.*, 74, 199-208, 2013.

Lang, J., Zhang, Y., Zhou, Y., Cheng, S., Chen, D., Guo, X., Chen, S., Li, X., Xing, X., Wang, H.: Trends of PM_{2.5} and chemical composition in Beijing, 2000-2015, *Aerosol Air Qual. Res.*, 17, 412-425, 2017.

Li, L. J., Ho, S. S. H., Feng, B., Xu, H., Wang, T., Wu, R., Huang, W., Qu, L., Wang, Q., and Cao, J.: Characterization of particulate-bound polycyclic aromatic compounds (PACs) and their oxidations in heavy polluted atmosphere: A case study in urban Beijing, China during haze events, *Sci. Tot. Environ.*, 660, 1392-1402, 2019.

Li, J., Du, H., Wang, Z., Sun, Y., Yang, W., Li, J., Tang, X., Fu, P.: Rapid formation of a severe regional winter haze episode over a mega-city cluster on the North China Plain, *Environ. Pollut.*, 223, 605-615, 2017

Lin, Y., Ma, Y., Qiu, X., Li, R., Fang, Y., Wang, J., Zhu, Y., Hu, D.: Sources, transformation, and health implications of PAHs and their nitrated, hydroxylated, and oxygenated derivatives in PM_{2.5} in Beijing, *J. Geophys. Res. Atmos.*, 120, 7219-7228, doi:10.1002/2015JD023628, 2015.

Lv, D., Chen, Y., Zhu, T., Li, T., Shen, F., and Li X.: The pollution characteristics of PM₁₀ and PM_{2.5} during summer and winter in Beijing, Suning and Islamabad, *Atmos. Pollut. Res.*, in press, <https://doi.org/10.1016/j.apr.2019.01.021>, 2019.

Lyu, R., Shi, Z., Alam, M. S., Wu, X., Liu, D., Vu, T. V., Stark, C., Fu, P., Feng, Y., and Harrison, R. M.: Alkanes and aliphatic carbonyl compounds in wintertime PM_{2.5} in Beijing, China, *Atmos. Environ.*, 202, 244-255, 2019.

Lyu, R., Alam, M. S., Stark, C., Xu, R., Shi, Z., Feng, Y., Harrison, R. M.: Aliphatic Carbonyl Compounds (C₈-C₂₆) in Wintertime Atmospheric Aerosol in London, UK, *Atmos. Chem. Phys.*, submitted, 2018a.

- Lyu, R., Shi, Z., Alam, M. S., Wu, X., Liu, D., Vu, T. V., Stark, C., Fu, P., Feng, Y., Harrison R. M.: Alkanes and aliphatic carbonyl compounds in wintertime PM_{2.5} in Beijing, China, *Atmos. Environ.*, submitted, 2018b.
- Ma, Y., Cheng, Y., Qiu, X., Cao, G., Fang, Y., Wang, J., Zhu, T., Yu, J., Hu, D.: Sources and oxidative potential of water-soluble humic-like substances (HULIS WS) in fine particulate matter (PM_{2.5}) in Beijing, *Atmos. Chem. Phys.*, 18, 5607-5617, 2018.
- Ma, Q., Wu, Y., Zhang, D., Wang, X., Xia, Y., Liu, X., Tian, P., Han, Z., Xia, X., Wang, Y., Zhang, R.: Roles of regional transport and heterogeneous reactions in the PM_{2.5} increase during winter haze episodes in Beijing, *Sci. Tot. Environ.*, 599-600, 246-253, 2017.
- Ogawa, H., Ibuki, T., Minematsu, T., Miyamoto, N.: Diesel combustion and emissions of decalin as a high productivity gas-to-liquid fuel, *Energy & Fuels*, 21, 1517-1521, 2007.
- Oliveira, T. S., Pio, C., Alves, C. A., Silvestre, A. J., Evtyugina, M., Afonso, J., Fialho, P., Legrand, M., Puxbaum, H., Gelencsér, A.: Seasonal variation of particulate lipophilic organic compounds at nonurban sites in Europe. *J. Geophys. Res.: Atmospheres*, 112., D23S09, doi:10.1029/2007JD008504, 2007.
- Oros, D., Simoneit, B.: Identification and emission rates of molecular tracers in coal smoke particulate matter, *Fuel* 79, 515-536, 2000.
- Pan, S., Wang, L.: Atmospheric oxidation mechanism of m-xylene initiated by OH radical, *J. Phys. Chem. A*, 118, 10778-10787, 2014.
- Pitts, J. N., Lokensgard, D. M., Ripley, P. S., Van Cauwenberghe, K. A., Van Vaeck, L., Shaffer, S. D., Thill, A. J., Belser, W. L.: Atmospheric epoxidation of benzo[a]pyrene by ozone: Formation of the metabolite benzo[a]pyrene-4, 5-oxide, *Science*, 210, 1347-1349, 1980.
- Ren, L., Fu, P., He, Y., Hou, J., Chen, J., Pavuluri, C.M., Sun, Y., Wang, Z.: Molecular distributions and compound-specific stable carbon isotopic compositions of lipids in wintertime aerosols from Beijing, *Scientific Rep.*, 6, 27481, 2016.
- Ringuet, J., Albinet, A., Leoz-Garziandia, E., Budzinski, H., Villenave, E.: Reactivity of polycyclic aromatic compounds (PAHs, NPAHs and OPAHs) adsorbed on natural aerosol particles exposed to atmospheric oxidants, *Atmos. Environ.*, 61, 15-22, 2012.
- Rogge, W. F., Hildemann, L. M., Mazurek, M. A., Cass, G. R., Simoneit, B. R.T ., Sources of Fine Organic Aerosol. 6. Cigaret Smoke in the Urban Atmosphere, *Environ.Sci.Technol.*, 28, 1375-1388, 1994.
- Rogge, W. F., Hildemann, L. M., Mazurek, M. A., Cass, G. R., Simoneit, B. R. T.: Sources of fine organic aerosol. 2. Noncatalyst and catalyst-equipped automobiles and heavy-duty diesel trucks, *Environ. Sci.Technol.*, 27, 636-651, 1993a.
- Rogge, W. F., Mazurek, M. A., Hildemann, L. M., Cass, G. R., Simoneit, B. R. T.: Quantification of urban organic aerosols at a molecular level: Identification, abundance and seasonal variation, *Atmos. Environ., Part A*, 27, 1309-1330, 1993b.

Ruehl, C. R., Nah, T., Isaacman, G., Worton, D. R., Chan, A. W. H., Kolesar, K. R., Cappa, C. D., Goldstein, A. H., and Wilson, K. R.: The Influence of molecular structure and aerosol phase on the heterogeneous oxidation of normal and branched alkanes by OH, *J. Phys. Chem. A.*, 117, 3990-4000, 2013.

Schauer, J. J., Cass, G. R.: Source apportionment of wintertime gas-phase and particle-phase air pollutants using organic compounds as tracers, *Environ. Sci. Technol.*, 34, 1821-1832, 2000.

Schauer, J. J., Rogge, W. F., Hildemann, L. M., Mazurek, M. A., Cass, G. R., Simoneit, B. R. T.: Source apportionment of airborne particulate matter using organic compounds as tracers, *Atmos. Environ.*, 30, 3837-3855, 1996.

Schmitter, J., Ignatiadis, I., Arpino, P.: Distribution of diaromatic nitrogen bases in crude oils, *Geochimica et Cosmochimica Acta*, 47, 1975-1984, 1983.

Schwantes, R. H., Schilling, K. A., McVay, R. C., Lignell, H., Coggon, M. M., Zhang, X., Wennberg, P. O., and Seinfeld, J. H.: Formation of highly oxygenated low-volatility products from cresol oxidation, *Atmos. Chem. Phys.*, 17, 3453-3474, 2017.

Shakya, K. M., Griffin, R. J.: Secondary organic aerosol from photooxidation of polycyclic aromatic hydrocarbons, *Environ. Sci. Technol.*, 44, 8134-8139, 2010.

Shen, R., Schäfer, K., Schnelle-Kreis, J., Shao, L., Norra, S., Kramar, U., Michalke, B., Abbaszade, G., Streibel, T., Zimmermann, R., Emeis, S.: Seasonal variability and source distribution of haze particles from a continuous one-year study in Beijing, *Atmos. Pollut. Res.*, 9, 627-633, 2018.

Shen, G., Tao, S., Wei, S., Zhang, Y., Wang, R., Wang, B., Wei, L.I., Shen, H., Huang, Y., and Chen, Y.: Emissions of parent, nitro, and oxygenated polycyclic aromatic hydrocarbons from residential wood combustion in rural China, *Environ. Sci. Technol.*, 46, 8123-8130, 2012a.

Shen, G., Wei, S., Zhang, Y., Wang, R., Wang, B., Li, W., Shen, H., Huang, Y., Chen, Y., and Chen, H.: Emission of oxygenated polycyclic aromatic hydrocarbons from biomass pellet burning in a modern burner for cooking in China, *Atmos. Environ.*, 60, 234-237, 2012b.

Shen, G., Tao, S., Wang, W., Yang, Y., Ding, J., Xue, M., Min, Y., Zhu, C., Shen, H., and Li, W.: Emission of oxygenated polycyclic aromatic hydrocarbons from indoor solid fuel combustion, *Environ. Sci. Technol.*, 45, 3459-3465, 2011.

Simoneit, B. R. T., Kobayashi, M., Mochida, M., Kawamura, K., Lee, M., Lim, H.-J., Turpin, B. J., Komazaki, Y.: Composition and major sources of organic compounds of aerosol particulate matter sampled during the ACE-Asia campaign, *J. Geophys. Res.: Atmospheres*, 109, D19S10, doi:10.1029/2004JD004598, 2004.

Simoneit, B. R.: Biomass burning - a review of organic tracers for smoke from incomplete combustion, *Appl. Geochem.*, 17, 129-162, 2002a.

Simoneit, B. R. T.: Biomass burning - a review of organic tracers for smoke from incomplete combustion, *Appl. Geochem.*, 17, 129-162, 2002b.

Simoneit, B., Rogge, W., Lang, Q., Jaffé, R.: Molecular characterization of smoke from campfire burning of pine wood (*Pinus elliottii*), *Chemosphere-Global Change Sci.*, 2, 107-122, 2000.

Simoneit, B. R. T., Sheng, G., Chen, X., Fu, J., Zhang, J., Xu, Y.: Molecular marker study of extractable organic matter in aerosols from urban areas of China, *Atmos. Environ.*, 25, 2111-2129, 1991.

Simoneit, B. R.: Application of molecular marker analysis to vehicular exhaust for source reconciliations, *Intl. J. Environ. Anal. Chem.*, 22, 203-232, 1985.

Simoneit, B. R. T.: Organic matter of the troposphere—III. Characterization and sources of petroleum and pyrogenic residues in aerosols over the western united states, *Atmos. Environ.*, (1967) 18, 51-67, 1984.

Simoneit, B. R., Mazurek, M. A.: Organic matter of the troposphere-II. Natural background of biogenic lipid matter in aerosols over the rural western united states, *Atmos. Environ.*, (1967) 16, 2139-2159, 1982.

Simoneit, B., Schnoes, H., Haug, P., Burlingame, A.: High-resolution mass spectrometry of nitrogenous compounds of the Colorado Green River Formation oil shale, *Chem. Geol.*, 7, 123-141, 1971.

Simpson, C. D., Paulsen, M., Dills, R. L., Liu, L. J. S., Kalman, D. A.: Determination of methoxyphenols in ambient atmospheric particulate matter: Tracers for wood combustion, *Environ. Sci. Technol.*, 39, 631-637, 2005.

Staples, C. A., Peterson, D. R., Parkerton, T. F., Adams, W. J.: The environmental fate of phthalate esters: a literature review, *Chemosphere*, 35, 667-749, 1997.

Sun, Y., Wang, Z., Fu, P., Yang, T., Jiang, Q., Dong, H., Li, J., Jia, J.: Aerosol composition, sources and processes during wintertime in Beijing, China, *Atmos. Chem. Phys.*, 13, 4577-4592, 2013.

Turpin, B. J., Lim, H.-J.: Species contributions to PM_{2.5} mass concentrations: Revisiting common assumptions for estimating organic mass, *Aerosol Sci. Technol.*, 35, 602-610, 2001.

Wang, J., Ho, S. S. H., Huang, R., Gao, M., Liu, S., Zhao, S., Cao, J., Wang, G., Shen, Z., and Han, Y.: Characterization of parent and oxygenated-polycyclic aromatic hydrocarbons (PAHs) in Xi'an, China during heating period: An investigation of spatial distribution and transformation, *Chemosphere*, 159, 367, 2016.

Wang, W.: Regional distribution and air-soil exchange of polycyclic aromatic hydrocarbons (PAHs) and their derivatives in Beijing-Tianjin area, Ph.D. Dissertation, Peking University, Beijing, China, 2010.

Wang, G., Kawamura, K., Lee, S., Ho, K., Cao, J.: Molecular, seasonal, and spatial distributions of organic aerosols from fourteen Chinese cities, *Environ. Sci. Technol.*, 40, 4619-4625, 2006.

- Wang, G., Kawamura, K.: Molecular characteristics of urban organic aerosols from Nanjing: A case study of a mega-city in China, *Environ. Sci. Technol.*, 39, 7430-7438, 2005.
- Wang, Z., Bi, X., Sheng, G., Fu, J.: Characterization of organic compounds and molecular tracers from biomass burning smoke in South China I: Broad-leaf trees and shrubs, *Atmos. Environ.*, 43, 3096-3102, 2009.
- Wei, S., Huang, B., Liu, M., Bi, X., Ren, Z., Sheng, G., and Fu, J.: Characterization of PM_{2.5}-bound nitrated and oxygenated PAHs in two industrial sites of South China, *Atmos. Res.*, 109, 76-83, 2012.
- Welthagen, W., Schnelle-Kreis, J., Zimmermann, R.: Search criteria and rules for comprehensive two-dimensional gas chromatography–time-of-flight mass spectrometry analysis of airborne particulate matter, *J. Chromatogr., A* 1019, 233-249, 2003.
- Wu, X., Vu, T. V., Shi, Z., Harrison, R. M., Liu, D., Cen, K.: Characterization and Source Apportionment of Carbonaceous PM_{2.5} Particles in China - A Review, *Atmos. Environ.*, 189, 187-212, 2018.
- Yao, L., Yang, L., Yuan, Q., Yan, C., Dong, C., Meng, C., Sui, X., Yang, F., Lu, Y., Wang, W.: Sources apportionment of PM_{2.5} in a background site in the North China Plain, *Sci. Tot. Environ.*, 541, 590-598, 2016.
- Yee, L. D., Kautzman, K. E., Loza, C. L., Schilling, K. A., Coggon, M. M., Chhabra, P. S., Chan, M. N., Chan, A. W. H., Hersey, S. P., Crounse, J. D., Wennberg, P. O., Flagan, R. C., Seinfeld, J. H.: Secondary organic aerosol formation from biomass burning intermediates: phenol and methoxyphenols, *Atmos. Chem. Phys.*, 13, 8019-8043, 2013.
- Zhang, H., Worton, D. R., Shen, S., Nah, T., Isaacman-VanWertz, G., Wilson, K. R., and Goldstein, A. H.: Fundamental time scales governing organic aerosol multiphase partitioning and oxidative aging, *Environ. Sci. Technol.*, 49, 9768-9777, 2015.
- Zhang, Y.-X., Shao, M., Zhang, Y.-h., Zeng, L.-M., He, L.-Y., Zhu, B., Wei, Y., Zhu, X.: Source profiles of particulate organic matters emitted from cereal straw burnings, *J. Environ. Sci.*, 19, 167-175, 2007.
- Zhang, Q., Anastasio, C., Jimenez-Cruz, M.: Water-soluble organic nitrogen in atmospheric fine particles (PM_{2.5}) from northern California, *J. Geophys. Res.: Atmospheres*, 107, D11, 4112, 10.1029/2001JD000870, 2002.
- Zhao, J., Peng, P. A., Song, J., Ma, S., Sheng, G., Fu, J.: Characterization of organic matter in total suspended particles by thermodesorption and pyrolysis-gas chromatography-mass spectrometry, *J. Environ. Sci.*, 21, 1658-1666, 2009.
- Zhou, J., Wang, T., Zhang, Y., Zhong, N., Medeiros, P. M., Simoneit, B. R. T.: Composition and sources of organic matter in atmospheric PM₁₀ over a two year period in Beijing, China, *Atmos. Res.*, 93, 849-861, 2009.

TABLE LEGENDS:

Table 1: Comparison of identified organic compounds with earlier studies in Beijing. Data from the present study are mean \pm s.d. for n = 33 samples.

Table 2: Molecular formula, diagnostic ions and average concentrations of hopanes identified in PM_{2.5}.

Table 3: Estimated average concentrations of unknown compounds (ng m⁻³) in each section of the chromatogram for haze and non-haze conditions.

FIGURE LEGENDS:

Figure 1: The percentages of the organic compound groups in the total identified organic compounds.

Figure 2: A comparison of organic compound groups between non-haze and haze days. The average total concentration of the identified group was calculated in the non-haze (13 days) and haze periods (20 days), respectively.

Figure 3: The distribution of concentrations of PAHs (shaded bars, 25%-first quartile, 75%-third quartile).

Figure 4: The molecular distributions of aliphatic hydrocarbons and other homologous series, including n-alkanes, branched alkanes, n-alkenes, carbonyl compounds (n-alkanals, n-alkan-2-ones, n-alkan-3-ones), n-alkanoic acid and alkanols on haze and non-haze days.

Figure 5: The molecular distributions of n-C_n-cyclohexane, alkyl-bicyclic-alkanes, alkyl-benzenes, n-C_n-benzenes, alkyl-furanones and alkyl-pyridines on haze and non-haze days.

Figure 6: The concentration (ng m⁻³) sum of identified and unknown organic compounds in each chromatogram image section during (a) non-haze and (b) haze days.

987 **Table 1:** Comparison of identified organic compounds with earlier studies in Beijing. Data from the
988 present study are mean \pm s.d. for n = 33 samples.

	Concentrations, ng m-3	
Compound name	Present	Previous study
n-alkanols		
1-Dodecanol	2.27±1.49	0.90 j;
1-Tetradecanol	24.2±88.9	3.00 j;
1-Hexadecanol	6.66±20.7	1.2 d; 6.30 j;
1-Octadecanol	1.69±1.65	3.1 d; 20.1 j;
1-Eicosanol	3.71±2.96	19.5 j;
		Σ n-alkanols (C ₁₄ -C ₃₀) = 1200 e;
n-alkanoic acids		
Hexanoic acid	1.80±1.54	30.4 i; 0.00 j;
Heptanoic acid	0.73±1.05	0.62 j;
Octanoic acid	2.97±2.56	29.6 i; 0.62 j;
Nonanoic acid	1.23±1.37	2.07 j;
Decanoic acid	22.8±25.2	6.4 d; 5.8 i; 1.24 j;
		Σ n-alkanoic acid (C ₁₂ -C ₂₄) = 40-11000 e; Σ n-alkanoic acid (C ₅ -C ₃₂) = 426 g; Σ n-alkanoic acid (C ₆ -C ₂₂) = 363 h;
Hopanes		
18 α (H)22,29,30-trisnorhopane	2.91±3.06	0.22 j;
17 α (H)-22,29,30-Trisnorhopane	1.56±2.74	2.75 a; 2.3 d; 0.5 i; 0.21 j;
17 α (H)21 β (H)-30-norhopane	9.92±7.63	7.19 a; 4.1 d;
17 β (H)21 α (H)-hopane(moretane)	5.77±6.12	1.32 j; 1.9 d;
17 α (H)21 β (H)-hopane	3.71±5.49	3.51 a; 3.2 d; 0.8 i; 1.54 j;
17 α (H)21 β (H)-homohopane(22R)	1.32±1.31	0.63 a; 1.2 d; 0.42 j;
17 α (H)21 β (H)-homohopane(22S)	0.83±0.93	2.94 a; 1.2 d; 0.63 j;
17 α (H),21 β (H)-bishomohopane(22S)	5.23±6.51	0.7 d;
17 α (H)21 β (H)-bishomohopane(22R)	1.41±1.73	0.7 d;
Subtotal	32.7±24.7	
PAHs		
Naphthalene (NAP, 2-rings)	6.03±4.52	0.22 b; 2.4 i;
Acenaphthylene (ACY, 2-rings)	12.7±9.93	0.065 b; 0.3 i;
Acenaphthene (ACE, 2-rings)	6.04±8.94	0.79 b; 0.51g; 0.3 i;
Fluorene (FLU, 3-rings)	16.6±13.0	1.18 b; 1.65g; 0.5 i; 15.6 j;
Phenanthrene (PHE, 3-rings)	8.59±8.49	14.0 b; 0.9 d; 1.1 e; 21.65 f; 30.3g; 0.9 i; 95.7 j;
Anthracene (ANT, 3-rings)	6.14±6.53	1.70 b; 3.3 d; 5.74g; 0.2 i; 52.3 j;
Pyrene (PYR, 4-rings)	18.9±18.2	22.3 b; 12 d; 0.58 e; 31.3 f; 64.4g; 1.0 i; 235 j;
Fluoranthene (FLT, 4-rings)	21.0±20.4	41.5 b; 11 d; 0.23 e; 31.8 f; 76.4g; 1.1 i; 222 j;
Chrysene (CHR, 4-rings)	25.5±19.3	21.8 b; 1.00 d; 1.00 e; 50.6 f; 62.7g; 1.3 i; 140 j;
Benz[a]anthracene (BaA, 4-rings)	17.6±14.6	23.5 b; 19 d; 43.4 f; 45.1g; 0.8 i; 62.9 j;

	Concentrations, ng m-3	
Compound name	Present	Previous study
Benzo[k]fluoranthene (BkF, 4-rings)	8.81±7.68	17.0 b; 8.3 d; 33.6g ; 0.7 i; 30.5 j;
Cyclopenta[cd]pyrene (CcP, 5-rings)	8.60±10.2	68.0 j;
Perylene (PER, 5-rings)	3.20±2.69	2.81 b; 14 d; 5.99g ; 0.2 i;
Benzo[b]fluoranthene (BbF, 5-rings)	38.5±31.8	34.0 b; 59 d; 33.1 f; 53.6g ; 2.3 i; 134 j;
Benzo[a]pyrene (BaP, 5-rings)	13.1±13.8	14.6 b; 14 d; 0.08 e; 40.2 f; 28.6g ; 1.1 i; 41.3 j;
Indeno[1,2,3-cd]pyrene (IcdP, 6-rings)	12.3±8.82	18.1 b; 15.2 d; 0.32 e; 40.9 f; 32.3g ; 1.2 i; 18.2 j;
Benzo[ghi]perylene (BghiP, 6-rings)	12.4±11.1	12.2 b; 12 d; 0.33 e; 22.2g ; 2.6 i; 59.0 j;
Benzo[e]pyrene (BeP, 5-rings)	15.4±10.3	12.4 b; 12 d; 0.65 e; 24.7g ; 1.3 i; 72.6 j;
Dibenzo [a,h]pyrene (DBA, 5-rings)	5.68±7.35	2.01 b; 3.1 d;
Benzo[ghi]fluoranthene (BghiF,5-rings)	15.1±15.8	0.08 e; 15.3 f;
O-PAHs		
Anthracenedione (AQ)	5.12±5.97	108 b;
7,12-Benz[a]anthracenequinone (BaAQ)	4.09±3.61	2.14 b;
Aceanthrenequinone (AceAntQ)	2.41±2.89	0.01b;
Phenanthraquinone (PQ)	1.45±1.08	0.13 b;
9-Fluorenone (9-FluQ)	3.78±4.01	28.3g ;
Alkylated-(PAHs & OPAHs)		
Pyrene, 1-methyl- (1-MePYR)	21.5±21.5	3.80 b
Phenanthrene, 1-methyl- (1-MePHE)	5.29±5.38	4.29 b
Retene	5.39±9.72	0.12 e; 0.5 i;
Ester		
Dibutyl phthalate (DBP)	16.9±15.5	21 d; 3.00 j;
Diethyl Phthalate (DEP)	2.67±2.91	3.5 d; 24.0 j;
Di(2-ethylhexyl)-phthalate (DEHP)	16.0±12.6	130 d;
Diisobutyl phthalate	49.7±43.2	22 d;
Dimethyl phthalate	2.58±2.80	1.5 d;
Biomarkers		
Levoglucosan	355±232	310 a; 790.3 c; 171 d; 78 h; 97.1 i; 830 j;
Phytone	14.7±11.7	0.9 j;
Phytane	1.94±1.05	2.3 i; 1.30 j;
Pristane	2.24±1.69	1.8 i; 0.67 j;
Other nitrogen compounds (Nitro, amine, heterocyclic compounds)		
Benzo[f]quinoline	4.40±4.66	3.10 j;
Isoquinoline	0.80±0.83	0.22 j;
Phenolic compounds		
1-Naphthalenol (1-OH-NAP)	1.56±5.61	0.22 b
2-Naphthalenol (2-OH-NAP)	1.15±1.21	2.74 b
2-Dibenzofuranol (2-OHDBF)	1.84±2.09	1.47 b

989 a. Beijing, PKU, Heating seasons (Ma et al., 2018);
 990 b. Beijing, PKU, Heating seasons (Lin et al., 2015);
 991 c. Beijing, China University of Geosciences (Beijing), winter (Shen et al., 2018);
 992 d. Beijing, winter of 2003 (Wang et al., 2006)
 993 e. Beijing, urban, June (Simoneit et al., 1991);
 994 f. Beijing, urban, haze period (Gao et al., 2016);
 995 f.g. Beijing, PKU, haze period (Li et al., 2019);
 996 g.h. Beijing, PKU, winter (Huang et al., 2006);
 997 h.i. Beijing, PKU, winter (He et al., 2006b)
 998 i.j. During the 2008 Beijing Olympic Games, PKU sites, (Guo et al., 2013);
 999 j.k. Beijing, urban, winter (Zhou et al., 2009);
 1000 Beijing, PKU, winter (Huang et al., 2006);
 1001

1002 **Table 2:** Molecular formula, diagnostic ions and average concentrations of hopanes identified in
1003 PM_{2.5}.
1004

Compounds		Molecular formula	Diagnostic ions	IAP, ng m ⁻³
18α(H)22,29,30-trisnorneohopane	Ts	C ₂₇ H ₄₆	191/370	2.91 ± 3.06
17α(H)-22,29,30-Trisnorhopane	Tm	C ₂₇ H ₄₆	191/370	1.56 ± 2.74
17α(H)21β(H)-30-norhopane	29αβ	C ₂₉ H ₅₀	191/398	9.92 ± 7.63
17β(H)21α(H)-hopane(moretane)	30βα	C ₃₀ H ₅₂	191/412	5.77 ± 6.12
17α(H)21β(H)-hopane	30αβ	C ₃₀ H ₅₂	191/412	3.71 ± 5.49
17α(H)21β(H)-homohopane(22R)	30αβ-22R	C ₃₁ H ₅₄	191/426	1.32 ± 1.31
17α(H)21β(H)-homohopane(22S)	30αβ-22S	C ₃₁ H ₅₄	191/426	0.83 ± 0.93
17α(H),21β(H)-bishomohopane(22S)	30αβ-22S	C ₃₂ H ₅₆	191/440	5.23 ± 6.51
17α(H)21β(H)-bishomohopane(22R)	30αβ-22R	C ₃₂ H ₅₆	191/440	1.41 ± 1.73

1005

1006 **Table 3:** Estimated average concentrations of unknown compounds (ng m^{-3}) in each section of the
1007 chromatogram for haze and non-haze conditions.
1008

Section	Characteristics of organic compounds	Non-haze		Haze	
		Total	Unidentified	Total	Unidentified
1	Low molecular weight: ➤ carbon numbers (n-alkanes) ≤ 17 ; ➤ monoaromatics;	802	546	911	632
2	Medium molecular weight: ➤ $17 < \text{carbon numbers (n-alkanes)} \leq 23$; ➤ Oxidized hydrocarbons (alkanals, alkanones);	334	137	483	147
3	Medium molecular weight: ➤ $23 < \text{carbon numbers (n-alkanes)} \leq 27$; ➤ Oxidized hydrocarbons (alkanals, alkanones);	573	215	1060	228
4	High molecular weight: ➤ carbon numbers (n-alkanes) ≥ 27 ;	351	188	730	320
5	Oxidized monoaromatics;	621	289	1309	985
6	2 rings PAHs	485	303	1556	879
7	3-6 rings PAHs and hopanes;	792	440	1337	774
Total		3958	2119	7385	3964

1009

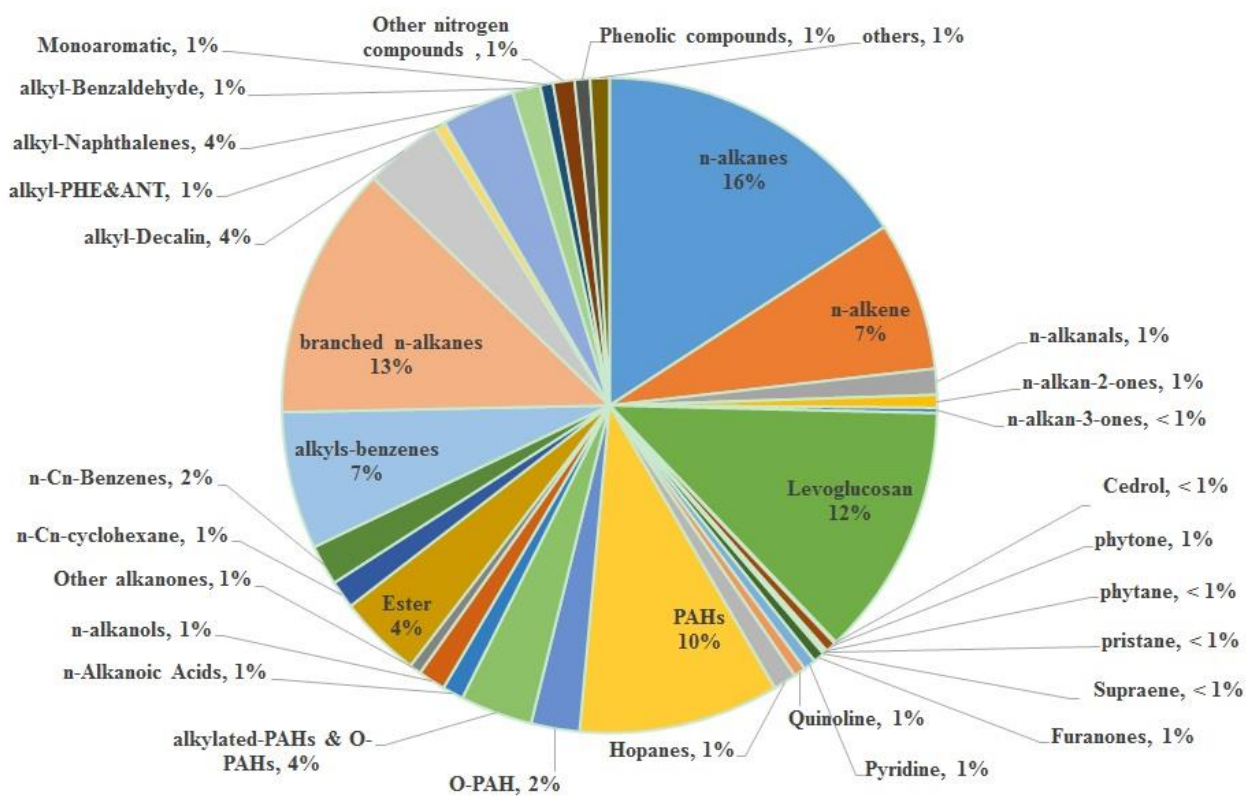
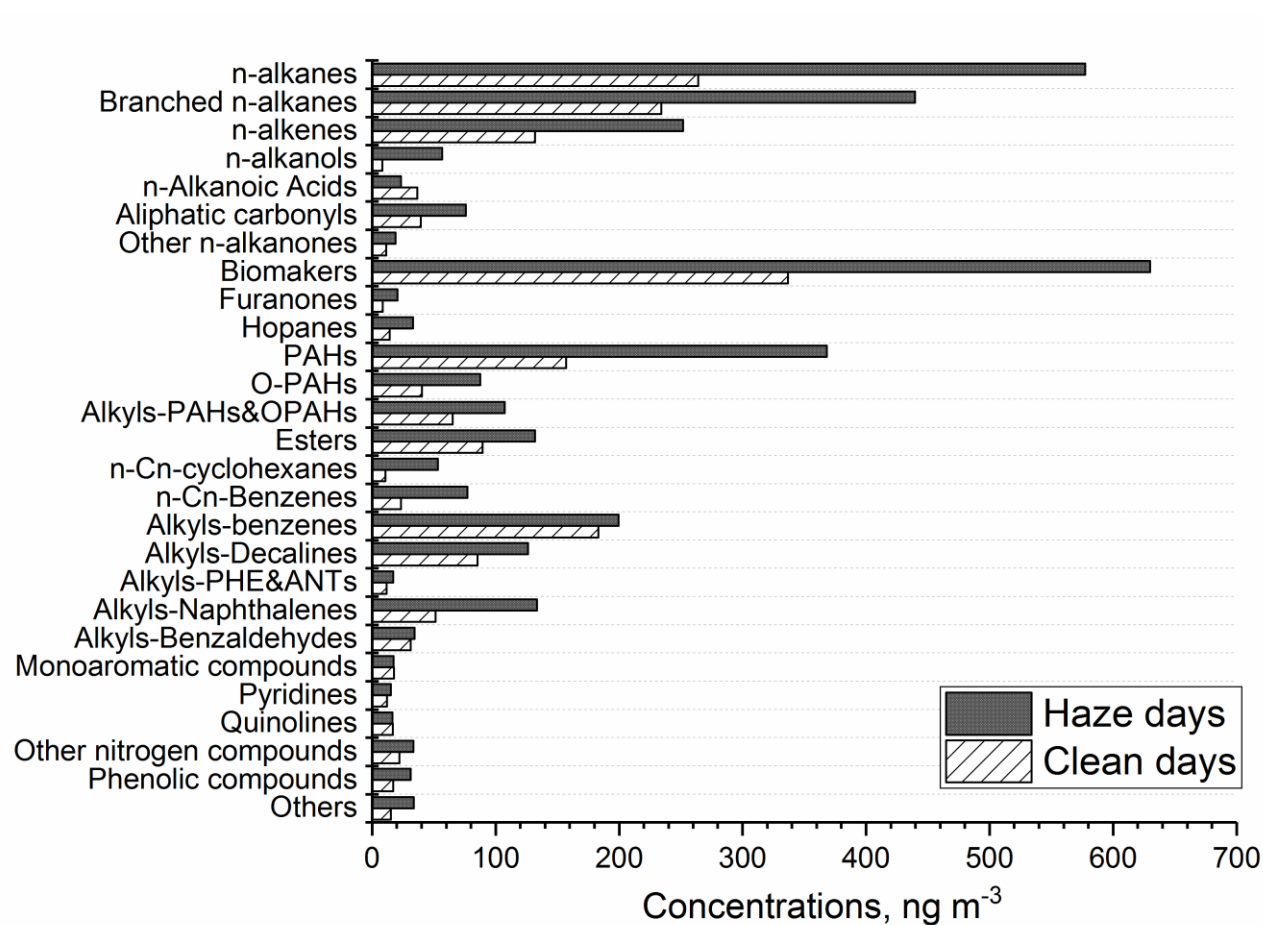


Figure 1: The percentages of the organic compound groups in the total identified organic compounds.

1013



1014

1015 **Figure 2:** A comparison of organic compound groups between non-haze and haze days. The average
1016 total concentration of the identified group was calculated in the non-haze (13 days) and haze periods
1017 (20 days), respectively.
1018

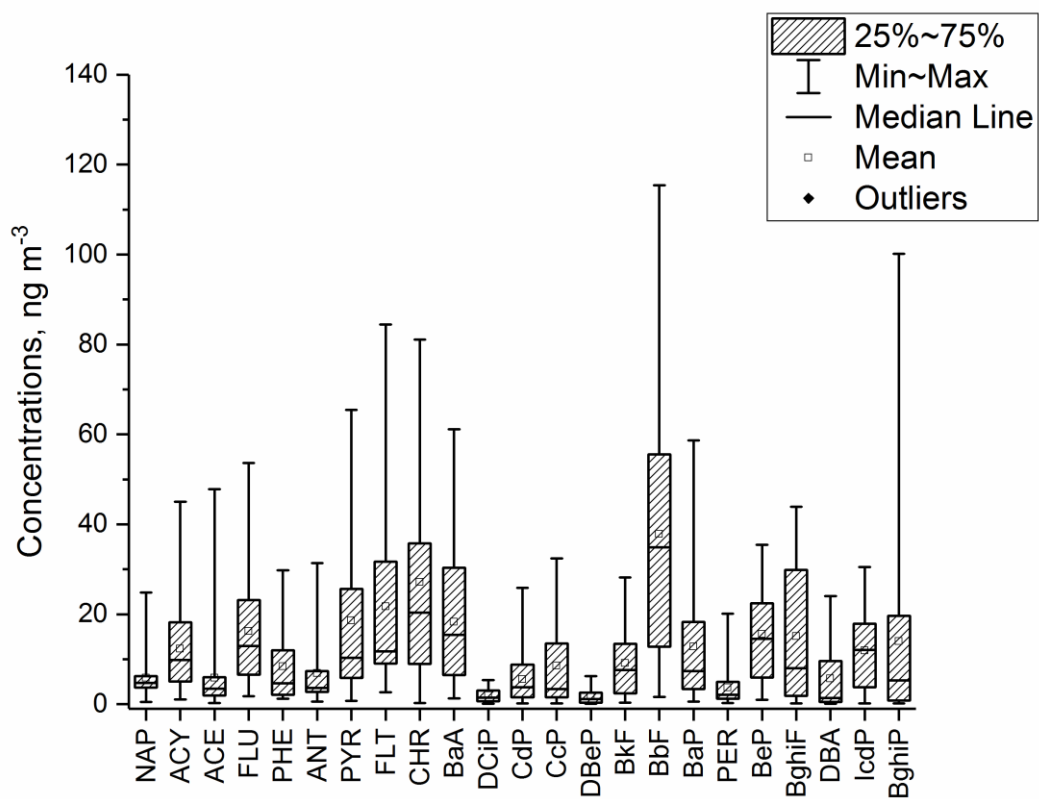


Figure 3: The distribution of concentrations of PAHs (shaded bars, 25%-first quartile, 75%-third quartile).

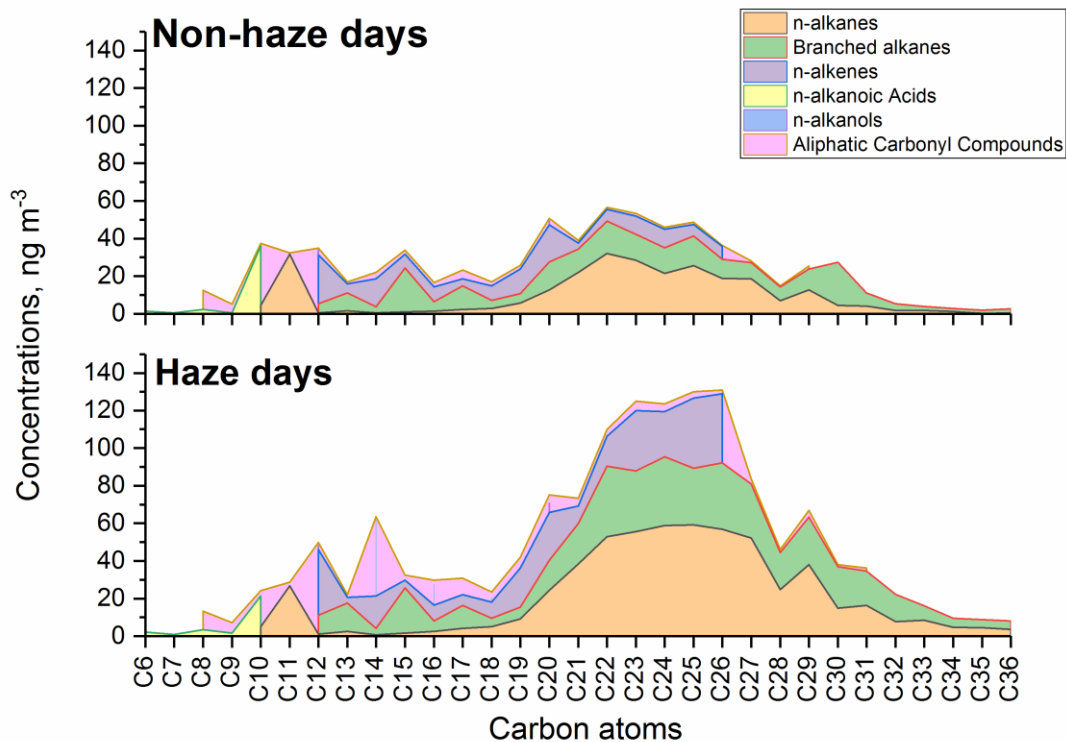
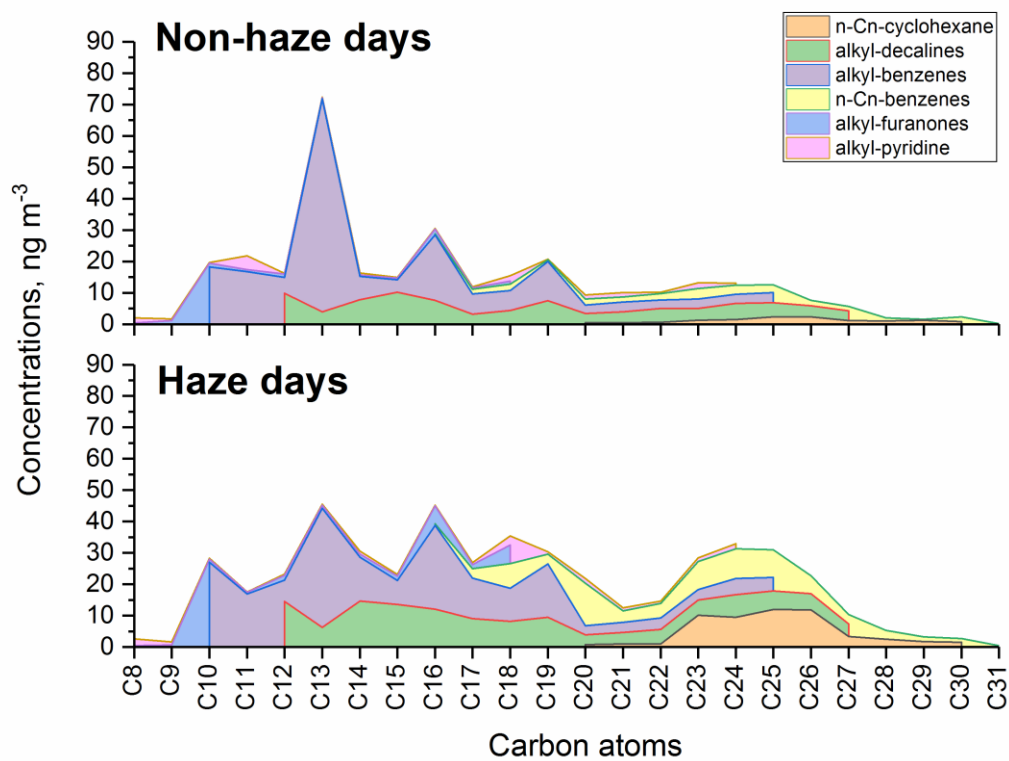


Figure 4: The molecular distributions of aliphatic hydrocarbons and other homologous series, including n-alkanes, branched alkanes, n-alkenes, carbonyl compounds (n-alkanals, n-alkan-2-ones, n-alkan-3-ones), n-alkanoic acid and alkanols on haze and non-haze days.



1030

1031

1032

1033

Figure 5: The molecular distributions of n-C_n-cyclohexane, alkyl-bicyclic-alkanes, alkyl-benzenes, n-C_n-benzenes, alkyl-furanones and alkyl-pyridines on haze and non-haze days.

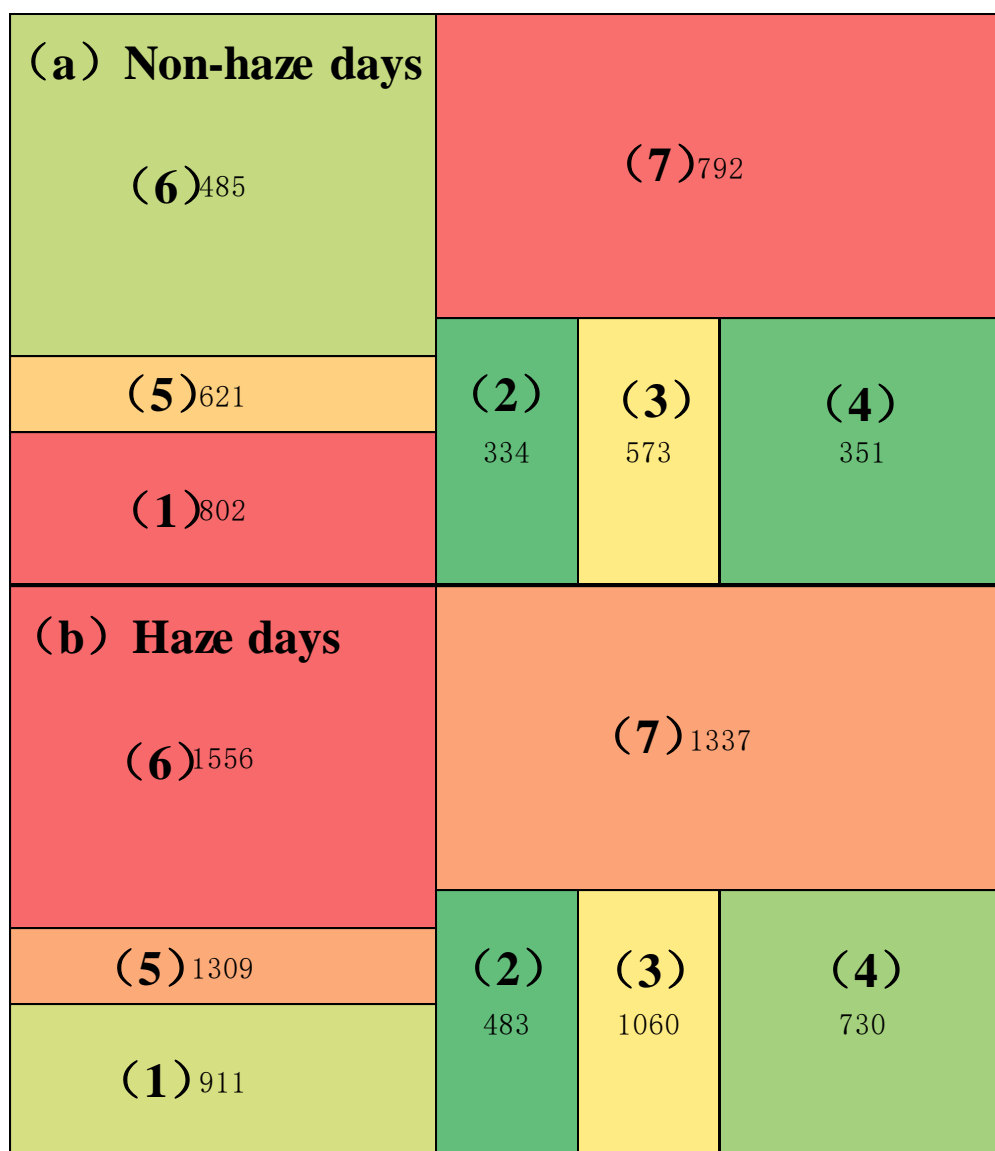


Figure 6: The concentration (ng m⁻³) sum of identified and unknown organic compounds in each chromatogram image section during (a) non-haze and (b) haze days.